Discontinuous Galerkin Method for Hyperbolic Conservation Laws

Thesis by

Ioanna Mousikou

In Partial Fulfillment of the Requirements

For the Degree of

Master of Science

King Abdullah University of Science and Technology

Thuwal, Kingdom of Saudi Arabia

November, 2016

EXAMINATION COMMITTEE PAGE

The thesis of Ioanna Mousikou is approved by the examination committee.

Committee Chairperson: Professor Athanasios Tzavaras
Committee Members: Professor Matteo Parsani, Professor Omar Knio

ABSTRACT

Discontinuous Galerkin Method for Hyperbolic Conservation Laws

Ioanna Mousikou

Hyperbolic conservation laws form a special class of partial differential equations. They describe phenomena that involve conserved quantities and their solutions show discontinuities which reflect the formation of shock waves. We consider one-dimensional systems of hyperbolic conservation laws and produce approximations using finite difference, finite volume and finite element methods. Due to stability issues of classical finite element methods for hyperbolic conservation laws, we study the discontinuous Galerkin method, which was recently introduced. The method involves completely discontinuous basis functions across each element and it can be considered as a combination of finite volume and finite element methods. We illustrate the implementation of discontinuous Galerkin method using Legendre polynomials, in case of scalar equations and in case of quasi-linear systems, and we review important theoretical results about stability and convergence of the method. The applications of finite volume and discontinuous Galerkin methods to linear and non-linear scalar equations, as well as to the system of elastodynamics, are exhibited.

ACKNOWLEDGEMENTS

I would like to express my gratitude to my advisors Prof. Athanasios Tzavaras and Prof. Theodoros Katsaounis for always being available to discuss my ideas and my thoughts. I greatly appreciated their guidance, their support and their assistance. A special thanks to my family and my friends for their encourage and their understanding during the last months.

TABLE OF CONTENTS

LIST OF FIGURES

LIST OF TABLES

Chapter 1

Introduction

Phenomena arising in science and engineering are commonly modelled by partial differential equations. In particular, phenomena involving conserved quantities are modelled by a special class of time-dependent partial differential equations, called conservation laws. Conservation laws are systems of partial differential equations in divergence form and they are usually considered as hyperbolic systems which implies additional properties. In one space dimension, the general form of such systems is

$$\frac{\partial}{\partial t}u(x,t) + \frac{\partial}{\partial x}f(u(x,t)) = 0, \tag{1.1}$$

where f is a function called flux function and u is a vector of the conserved variables; for example mass, momentum and energy. Imposing some initial conditions to equation (1.1), a Cauchy problem is obtained. However, the solvability of such problem cannot be assured despite the smoothness of initial conditions. In fact, solutions to hyperbolic conservations laws might develop discontinuities even for smooth initial condition and thus solutions cannot be defined globally in a classical sense, [1]. Accordingly, the concept of weak solutions is introduced which allows to consider as solutions functions of less regularity, admitting in particular discontinuities. However less regularity of weak solutions leads to multiple solutions for the Cauchy problem. To obtain uniqueness, an additional condition is imposed for selecting the physically correct solution. This condition, which reflects the physical origin of such systems, is called entropy condition and the weak solution which satisfies this condition is called

the entropy solution, [2] .

The wide range of applications of hyperbolic conservations laws led to a significant development of research in the field. The development of theoretical research caused early on to introduce methods for accurate and efficient approximations to the solutions of such problems, for example to compressible Euler equations, to shallow water equations as well as to Burgers' equations. Historically, finite difference methods were the first methods used to produce approximations of the solutions of hyperbolic conservation laws. The idea of these methods is to replace the continuous derivatives of the unknown functions by their finite difference approximations, [3].

The application of the finite difference methods to problems with realistic geometries is rather cumbersome, thus making the method not very attractive for realistic problems. This caused the need of other methods with more flexibility, such as finite volume and finite element methods. Finite volume methods produce approximations to the average of the solution across smaller domains and due to their construction, they are conservative and mimic the behaviour of the exact solution, [4], [5]. Thus, they became quite popular and used widely in recent years. By contrast, the Finite Element method follows a completely different approach to produce approximations of the solution. The idea consists of dividing the domain into smaller domains and replacing the solution by piecewise approximations produced by a finite set of continuous functions, [6]. Although it is a popular method for approximating solutions of elliptic and parabolic problem, the method in its classical form cannot be used for solving hyperbolic conservation laws since its applications leads to nonconservative methods which can be also unstable.

Recently, finite element methods found application to hyperbolic conservation laws in the form of the discontinuous Galerkin method. The original discontinuous Galerkin method was proposed in 1973 by Reed and Hill for solving steady-state neutron transport equations [7] and later on it has been extended for solving linear

and nonlinear time-dependent equations. The discontinuous Galerkin scheme for nonlinear scalar conservation laws was introduced in 1982 [8] involving the forward Euler method for time discretisation. However it was stable under a very strict condition and thus, a slope limiter was provided [9]. In 1989, a more accurate scheme was introduced using Runge-Kutta methods for time discretisation [10]. The Runge-Kutta discontinuous Galerkin method involved also a modified slope limiter which did not affect the accuracy on smooth regions. Later on, this concept was generalised for higher order Runge-Kutta schemes [11] and in multidimensional cases [12]. Slope limiters were further modified in [13], [14] and in the last decade ENO, WENO [15] and Hermite WENO [16] schemes are used as slope limiters. Lately, discontinuous Galerkin method was extended to problems with higher order spatial derivatives which are not necessarily hyperbolic. For example, local discontinuous Galerkin method was applied for convection-diffusion problems [17] and hybridisable discontinuous Galerkin method was applied for second order elliptic equations [18].

The fundamental difference between the discontinuous Galerkin method and the classical finite element method relies on the continuity of basis functions. In comparison with the classical finite element method, here the basis functions are completely discontinuous across each element interface and they consist of local piecewise polynomials. Due to the piecewise discontinuity of basis functions, the discontinuous Galerkin method can be applied locally in each element. This simplifies the implementation of the method, since the mass matrix becomes block diagonal and the solution of a large systems is avoided. In addition, the discontinuity across each element implies the existence of different degrees of freedom in each element independent of their neighbours, which is not allowed in classical finite element method. Consequently, we can easily apply adaptivity strategies by increasing the degrees of freedom near discontinuities to obtain better approximations to the solution.

Another important characteristic of the discontinuous Galerkin method can be

considered the treatment of boundary conditions which merges the finite element method with finite volume method. Motivated by the finite volume method, boundary terms of the problem are approximated by a consistent, monotone and Lipschitz continuous numerical flux. This ensures that the scheme we obtain is conservative, which does not hold in case of the classical finite element method.

The main purpose of this thesis is to build a solid background in the field of numerical analysis for solving hyperbolic conservation laws, by reviewing the fundamental numerical methods for hyperbolic conservation laws, and be equipped with the essential knowledge for further research in this field. We emphasise on the discontinuous Galerkin method, since it is considered as one of the most powerful and fastest growing methods with application in various problems, not necessarily hyperbolic. The discontinuity of basis functions, which implies further flexibility and additional properties, makes the method very attractive especially for handling discontinuities and realistic geometries. Therefore, it is reasonable to apply the method in order to produce approximations to the solutions of more complex problems in multi-dimension space, although the information for this area is limited. Hence, this thesis can be considered as the introductory step for applying the discontinuous Galerkin method for realistic problems in more than one dimension.

The thesis is organised in the following way: in Chapter 2, we give a brief introduction to the theory of conservation laws by summarising the fundamental properties and presenting some important examples. In Chapter 3, we review the finite difference, the finite volume and the finite element methods for one-dimension scalar hyperbolic conservation law. In the same chapter, we present the discontinuous Galerkin method and its implementation for nonlinear scalar hyperbolic conservation law and for systems of conservation laws. Finally, in Chapter 4 we review some important theoretical results about the stability and convergence of discontinuous Galerkin method and we exhibit numerical tests for one-dimensional examples.

Chapter 2

Conservation Laws

In this chapter, we give a brief introduction to hyperbolic conservation laws, we summarise their fundamental properties and we present some one-dimensional examples. Such systems might have discontinuities which reflects the existence of shock waves and due to these discontinuities classical solutions do not generally exist. Hence, we introduce the concept of weak solutions and present the entropy conditions in order to obtain uniqueness of the solution. For a complete presentation on the subject of Conservation Laws, we refer to [1] and [2] .

2.1 Introduction

Conservation laws is a special class of time-dependent systems of partial differential equations in divergence form. These systems of equations describe phenomena arising in mathematical physics. They were first studied in nineteenth century, in consequence of the study of gas dynamics. The general form of such system is

$$\frac{\partial}{\partial t}U(x,t) + \sum_{i=1}^{d} \frac{\partial}{\partial x_i} F_i(U(x,t)) = 0, \tag{2.1.1}$$

where $U : \mathbb{R}^d \times \mathbb{R}_+ \to \mathbb{R}^N$ is the vector of conserved variables; for example mass, momentum and energy. The function $F = (F_1, F_2, \ldots, F_d) : \mathbb{R}^N \to \mathbb{R}^{N\times d}$ is called the flux function. A vector U can be considered as the classical solution of (2.1.1) in $\mathbb{R}^N$ if it satisfies the system (2.1.1) and some additional initial conditions for every $(x,t) \in \mathbb{R}^d \times \mathbb{R}_+$ and the derivatives are understood in the classical sense.

Systems of conservation laws are mainly hyperbolic. The system (2.1.1) is called hyperbolic if for all $\nu \in \mathbb{R}^d$, $|\nu| = 1$, the Jacobian matrix of flux function,

$$\nu \cdot F'(U) = \sum_{i=1}^{d} \nu_i \frac{\partial F_i}{\partial U}(U), \tag{2.1.2}$$

has N real eigenvalues, $\lambda_1(U) \leq \lambda_2(U) \leq \cdots \leq \lambda_N(U)$ called characteristic speeds, and a complete set of eigenvectors for each U. If, in addition, the eigenvalues are distinct, then the system is strictly hyperbolic. Hyperbolicity implies that information propagates at a finite speed and the domain of dependence of each equation is always a bounded interval. In the sequel, we focus only on one dimensional (d=1) hyperbolic conservation laws.

2.2 Examples of hyperbolic conservation laws

Let us present some important examples of hyperbolic conservation laws arising in continuum physics.

1. Linear advection equation:

   The linear advection or transport equation is the simplest example of scalar conservation law. The equation takes the form

   $$u_t + \alpha u_x = 0, \qquad \alpha \in \mathbb{R}. \tag{2.2.1}$$

   The constant α denotes the wave propagation speed. Given an initial condition

   $$u(x,t) = u_0(x), \qquad x \in \mathbb{R},$$

   we can easily compute the exact solution by the method of characteristics and the solution is

   $$u(x,t) = u_0(x - \alpha t), \qquad t \geq 0. \tag{2.2.2}$$

2. Burgers' equation - Inviscid Burgers' equation:

   The Burger's equation is a nonlinear scalar hyperbolic conservation law given by

$$\frac{\partial}{\partial t}u(x,t) + \frac{\partial}{\partial x}f(u(x,t)) = 0, \tag{2.2.3}$$

   where $f(u) = \frac{1}{2}u^2$. In general, a nonlinear scalar equation is hyperbolic if $f''(u) \neq 0$. The Burgers' equation arises from fluid dynamics and it can be considered as a simplified model of incompressible Navier - Stokes equations. Actually the equation studied by Burger,[19], includes viscosity, involving a second spatial derivative term. Hence, we refer to (2.2.3) as the inviscid Burger's equation.

3. Wave equation:

   The wave equation is a well known partial differential equation given by

$$u_{tt} - c^2 u_{xx} = 0, \qquad c \in \mathbb{R}. \tag{2.2.4}$$

   However, it can be rewritten as a linear hyperbolic system of conservation laws taking the form

$$\frac{\partial}{\partial t}\begin{bmatrix} v \\ w \end{bmatrix} + \frac{\partial}{\partial x}\begin{bmatrix} -w \\ -c^2 v \end{bmatrix} = 0, \tag{2.2.5}$$

   where $v = u_x$ and $w = u_t$.

   In general, a linear system $u_t + Au_x = 0$ is hyperbolic if the matrix A, consisting of real constant values independent of x, has real eigenvalues and it is diagonalisable.

4. Compressible Euler equations:

   The compressible Euler equations of gas dynamics is a nonlinear system of hyperbolic conservation laws which is widely used in the field of fluid dynamics.

The equations correspond to the conservation of mass, momentum and energy of the gas respectively and take the form

$$\frac{\partial}{\partial t}\begin{bmatrix}\rho\\ \rho u\\ E\end{bmatrix}+\frac{\partial}{\partial x}\begin{bmatrix}\rho u\\ \rho u^2+p\\ u(E+p)\end{bmatrix}=0, \tag{2.2.6}$$

where ρ is the density, u is the velocity with $\rho u = m$ the momentum, E is the total energy and p is the pressure of the gas. In N space dimensions, the system (2.2.6) can be extended to the following

$$\begin{cases}\rho_t+\nabla\cdot(\rho u)=0,\\ (\rho u)_t+\nabla\cdot(\rho u\otimes u)+\nabla p=0,\\ E_t+\nabla\cdot((E+p)\,u)=0,\end{cases} \tag{2.2.7}$$

where $u\in\mathbb{R}^N$ is the velocity vector and p is the pressure.

5. System of Elastodynamics in one-dimension:

The system of elastodynamics is a special case of Euler equation, where the conservation of energy is omitted. It describes the propagation of an elastic wave in a medium. The system consists of two equations, a linear and nonlinear conservation law

$$\begin{cases}u_t-v_x=0,\\ v_t-g(u)_x=0,\end{cases} \tag{2.2.8}$$

where u is the shear-strain, v is the velocity and $g(u)$ is a convex function, i.e. $g''(u)>0$, describing the stress. In divergence form, the system (2.2.8) is given by

$$\frac{\partial}{\partial t}\begin{bmatrix}u\\ v\end{bmatrix}+\frac{\partial}{\partial x}\begin{bmatrix}-v\\ -g(u)\end{bmatrix}=0. \tag{2.2.9}$$

2.3 Shock Formation

Solutions to hyperbolic conservation laws may exhibit discontinuities. In particular, at a finite time, solutions may be discontinuous and cannot be defined globally even for smooth initial data. We illustrate this behaviour by considering the scalar equation

$$\frac{\partial}{\partial t}u(x,t) + \frac{\partial}{\partial x}f(u(x,t)) = 0, \qquad x \in \mathbb{R}, \tag{2.3.1}$$

with smooth initial condition,

$$u(x,t) = u_0(x), \qquad u_0 \in C^1(\mathbb{R}).$$

Let the flux function f be $C^2(\mathbb{R})$. For small time, the associated characteristics passing through the point $(\xi, 0)$ satisfy the following

$$\begin{cases} x'(t) = f'(u(x,t),t), \\ x(0) = \xi. \end{cases} \tag{2.3.2}$$

Since

$$\frac{d}{dt}u(x,t) = \frac{\partial u}{\partial t} + \frac{\partial u}{\partial x}x'(t) = \frac{\partial u}{\partial t} + \frac{\partial u}{\partial x}f'(u(x,t),t) = 0,$$

we conclude that the solution $u(x,t)$ is constant along the characteristics. Therefore, from (2.3.2), we obtain the characteristic curve passing through the point $(\xi, 0)$

$$x = \xi + tf'(u_0(\xi))). \tag{2.3.3}$$

It follows that the solution, for small t, is given by

$$u(x,t) = u(\xi,0) = u_0(\xi) = u_0(x - tf'(u)). \tag{2.3.4}$$

Although the solution (2.3.4) is obtained by the method of characteristics, it does not imply that it is valid globally.

Let consider the case where two characteristic curves cross. The intersection of the characteristics yields that $u(x,t)$ takes two different values at some point and it implies that $u(x,t)$ is necessarily discontinuous. The discontinuity is called shock. Let us examine when the characteristics cross and a shock is formed.

Proposition 2.3.1. Let (2.3.1) be a scalar conservation law and (2.3.2) be the characteristic curves of (2.3.1). The characteristics cross if

$$\frac{d}{dt}f'(u_0(x)) < 0, \qquad \text{at any } x \in \mathbb{R}. \tag{2.3.5}$$

The shock occurs at time

$$T_b = \frac{-1}{\min_{x\in\mathbb{R}} \frac{d}{dt}f'(u_0(x))}. \tag{2.3.6}$$

Proof. Firstly, we examine when the characteristics cross. We assume that there exist two points $\xi_1(t) = \xi_1$ and $\xi_2(t) = \xi_2$, $\xi_1 < \xi_2$, such that their characteristic curves cross at time t. From (2.3.3), it follows

$$\xi_1 + tf'(u_0(\xi_1))) = \xi_2 + tf'(u_0(\xi_2))).$$

Solving for t leads to

$$t = \frac{\xi_1 - \xi_2}{f'(u_0(\xi_2))) - f'(u_0(\xi_1)))}.$$

We set $h = \xi_2 - \xi_1$ and let $h \to 0$, then

$$t = \lim_{h\to 0} \frac{-h}{f'(u_0(\xi_1 + h))) - f'(u_0(\xi_1)))} = \frac{-1}{\frac{d}{dt}f'(u_0(x))}.$$

Thus, the characteristics cross for the first time at

$$T_b = \frac{-1}{\min_{x\in\mathbb{R}} \frac{d}{dt} f'(u_0(x))}. \tag{2.3.7}$$

Let examine now if (2.3.5) is a necessary condition for intersecting characteristics. Considering that u becomes discontinuous when the characteristics cross, we check the differentiability of u, at $t = T_b$. We take

$$\frac{\partial}{\partial x} u(x,t) = \frac{u_0'(x)}{1 + t u_0(x)' f''(u_0(x))} = \frac{u_0'(x)}{1 + t \frac{d}{dt} f'(u_0(x))}. \tag{2.3.8}$$

We observe that u is not differentiable if for some x, $\frac{d}{dt} f'(u_0(x)) < 0$,

$$\lim_{t\to T_b} \frac{\partial}{\partial x} u(x,t) = \lim_{t\to T_b} \frac{u_0'(x)}{1 + t \frac{d}{dt} f'(u_0(x))} = \infty. \tag{2.3.9}$$

Hence, (2.3.5) is a necessary condition for intersecting characteristics.

From proposition (2.3.1), we obtain that beyond a shock, i.e. for $t > T_b$, u is no longer differentiable and implies that the solution is determined only in a weak sense.

2.3.1 Shock speed

Let $u(x,t)$ denotes a discontinuous solution of (2.3.1) and let u_- and u_+ be the corresponding values to the left and the right of the discontinuity. The propagating speed of the discontinuity is called shock speed, s, and is given by Rankine - Hugoniot jump condition,

$$f(u_-) - f(u_+) = s(u_- - u_+). \tag{2.3.10}$$

2.4 Weak solutions

As we have seen before, due to discontinuities, the solution of hyperbolic conservation laws cannot be defined globally in the classical sense. Here we introduce the concept

of weak solutions.

We consider again the equation (2.3.1) and let $\phi(x,t) \in C_c^\infty(\mathbb{R} \times \mathbb{R}_+)$, be a test function. We multiply (2.3.1) by $\phi(x,t)$ and then integrate over space and time. Then,

$$\int_0^\infty \int_{\mathbb{R}} \phi \left(u_t + f(u)_x\right) dxdt = 0. \tag{2.4.1}$$

Integrating by parts over space and time, we obtain

$$\int_{\mathbb{R}} \phi(x,0)u(x,0)dx + \int_0^\infty \int_{\mathbb{R}} \left(\phi_t u + \phi_x f(u)\right) dxdt = 0. \tag{2.4.2}$$

Let us introduce the following definition.

Definition 2.4.1. A function $u(x,t) \in L^\infty(\mathbb{R})$ is a weak solution of the hyperbolic conservation law (2.3.1) if for any $\phi(x,t) \in C_c^\infty(\mathbb{R} \times \mathbb{R}_+)$, (2.4.2) holds.

In general, weak solutions are not unique and some additional criteria are required to obtain uniqueness.

2.5 Entropy conditions

Due to the lack of uniqueness for weak solutions, an additional condition is imposed for selecting the physically correct solution. This condition is related to the entropy property which reflects the physics of the problem. The condition is called entropy condition and the weak solution which satisfies this condition is called the entropy solution.

Let u be a weak solution of the hyperbolic conservation law (2.3.1) and let u_- and u_+ denote the corresponding values to the left and the right of a shock. Then u is the entropy solution to (2.3.1) if satisfies one of the following form of entropy condition.

- Entropy condition I - Lax's entropy condition:

The shock speed s provided by Rankine-Hugoniot jump condition satisfies

$$f'(u_-) > s > f'(u_+). \tag{2.5.1}$$

If f is convex, $f''(u) \geq 0$, then the condition reduces to $u_- > u_+$. For non-convex flux functions, a different notion of entropy is given by

- Entropy condition II - Oleinik's entropy condition:

  All discontinuities satisfy

$$\frac{f(u) - f(u_-)}{u - u_-} \geq s \geq \frac{f(u) - f(u_+)}{u - u_+}, \tag{2.5.2}$$

  for all u between u_- and u_+. The Oleinik's condition implies Lax's condition but the converse is not necessarily correct. The Lax's condition is equivalent to Oleinik's condition if and only if f is strictly convex, i.e. $f''(u) > 0$.

Besides the notion of entropy for shock waves, there is another form of entropy condition for rarefaction fans. Let us explain first when a rarefaction fan does occur. Consider a hyperbolic conservation law (2.3.1) with f is convex and discontinuous initial data, i.e. a Riemann problem. A rarefaction fan occurs when the propagating speed before the discontinuity is less than the speed after the discontinuity, i.e. $u_- < u_+$. In this case, if $u(x,t)$ is an increasing function in x then there is a region where the characteristics are spread out in various ways and hence, there exist infinite many weak solutions. By quantifying the rate of spreading [20], we obtain that u is the entropy solution to (2.3.1) if it satisfies the following condition

- Entropy condition III :

  There exists a constant $M > 0$ such that

$$\frac{u(x+c,t) - u(x,t)}{c} < \frac{M}{t}, \qquad \forall c > 0, t > 0 \text{ and } x \in \mathbb{R}. \tag{2.5.3}$$

This implies that $u(\cdot, t)$ as a function of t has local bounded total variation [21]. If we consider that $c = \Delta x$, then this formulation can be also applied in case of discrete problems

$$|U_{j+1}(t) - U_j(t)| < \frac{M}{t}\Delta x.$$

and it provides that U_j has local bounded total variation.

Chapter 3

Numerical Methods for Hyperbolic Conservation Laws

In this chapter we review briefly numerical methods for hyperbolic conservation laws. For simplicity of the presentation we consider only one dimensional scalar hyperbolic conservation laws as well as linear hyperbolic systems.

The development of theoretical research in the field of hyperbolic conservations laws led early on to the introduction of methods that produce numerical approximation to the solutions of such problems. Historically, finite difference methods were the first methods used to produce approximations to solutions of hyperbolic conservation laws. However, the application of the finite difference methods to problems with realistic geometries is rather cumbersome, thus making the method not very attractive. Hence other methods with more flexibility, such as finite volume and finite element methods, were introduced. Finite volume methods became quite popular in recent years and they are widely used in fluid dynamic problems. The finite element method, although is a popular method for approximating solutions of elliptic and parabolic problem, only recently found application to hyperbolic conservation laws in the form of the discontinuous Galerkin method. The numerical methods are fully presented in references [3], [4],[22],[6] [23] and [24].

Let us introduce the finite difference methods for a one - dimensional linear hyperbolic conservation law.

3.1 Finite Difference Methods

The fundamental idea of finite difference methods is replacing the continuous derivatives of the unknowns functions by their finite difference approximations to produce approximations to the solution at discrete points, [3]. Here we develop the method on a simple example of linear transport equation.

We consider the Cauchy problem

$$\begin{cases} u_t + \alpha u_x = 0, & x \in \mathbb{R}, t \geq 0, \alpha \in \mathbb{R}, \\ u(x,0) = u_0(x). \end{cases} \tag{3.1.1}$$

We introduce a uniform mesh of fixed width Δx and a discretisation in time of fixed time step Δt. The discrete points (x_j, t_n) are defined by

$$x_j = j\Delta x, \quad j = \ldots, -1, 0, 1, 2, \ldots$$
$$t_n = n\Delta t, \qquad n = 0, 1, 2, \ldots$$

Let us denote

$$U_j^n \approx u(x_j, t_n), \tag{3.1.2}$$

the approximate solution at the grid point (x_j, t_n). Then a possible discretisation of (3.1.1) is to consider the forward difference approximation in space and time

$$u_x(x_j, t_n) \approx \frac{U_{j+1}^n - U_j^n}{\Delta x}, \qquad u_t(x_j, t_n) \approx \frac{U_j^{n+1} - U_j^n}{\Delta t}. \tag{3.1.3}$$

From (3.1.3) and (3.1.1), we obtain the one-sided finite difference schemes

$$\frac{U_j^{n+1} - U_j^n}{\Delta t} + \alpha \frac{U_{j+1}^n - U_j^n}{\Delta x} = 0, \qquad \forall j, \forall n. \tag{3.1.4}$$

Equivalently, we can rewrite (3.1.4) in an explicit form

$$U_j^{n+1} = U_j^n - \alpha\frac{\Delta t}{\Delta x}(U_{j+1}^n - U_j^n), \qquad j \in \mathbb{Z}, n = 0, 1, \ldots \tag{3.1.5}$$

Considering that (3.1.1) models a wave propagation with speed α, it follows that the direction the solution of (3.1.1) is moving is determined by the sign of α. This means that if $\alpha > 0$, the solution propagates to the right and if $\alpha < 0$, then the solution propagates to the left. Hence a proper upwind scheme should depend on the sign of α. Indeed, the scheme (3.1.5) is appropriate for $\alpha < 0$. The corresponding upwind scheme in the case of $\alpha > 0$ is

$$U_j^{n+1} = U_j^n - \alpha\frac{\Delta t}{\Delta x}(U_j^n - U_{j-1}^n), \qquad j \in \mathbb{Z}, n = 0, 1, \ldots \tag{3.1.6}$$

Thus, by combining these two results, (3.1.5) and (3.1.6), we can derive a composite form of the upwind scheme

$$U_j^{n+1} = U_j^n - \frac{\Delta t}{\Delta x}(\alpha^+ U_x^{n,-} + \alpha^- U_x^{n,+}), \tag{3.1.7}$$

where

$$\alpha^+ = \max(\alpha, 0), \qquad \alpha^- = \min(\alpha, 0) \tag{3.1.8}$$

and

$$U_x^{n,-} = U_j^n - U_{j-1}^n, \qquad U_x^{n,+} = U_{j+1}^n - U_j^n. \tag{3.1.9}$$

Similarly, we can derive finite difference schemes for nonlinear hyperbolic conservation laws. However the nonlinearity of the flux functions raises further difficulties. For example a method may converge to a weak solution of the conservation laws but not to the entropy solution.

3.1.1 CFL condition

It was shown by Courant, Friedrichs and Lewy that a numerical method is stable and thus converges to the entropy solution if the numerical domain of dependence contains the true domain of dependence of the partial differential equation which is applied for. This is considered as the CFL condition and it is a necessary but not sufficient condition to obtain stability [3]. We note that a method is defined to be stable if the error does not grow exponentially in time. For a hyperbolic conservation law, the CFL condition can be considered as the following ratio:

$$\lambda \frac{\Delta t}{\Delta x} \leq 1, \tag{3.1.10}$$

where $\lambda = \max_u |f'(u)|$. In case of linear scalar hyperbolic conservation laws, i.e. if $f(u) = \alpha u$, the CFL condition is simplified to

$$\alpha \frac{\Delta t}{\Delta x} \leq 1. \tag{3.1.11}$$

Consequently, the finite difference scheme (3.1.7) is stable and convergent if the CFL condition is satisfied.

3.2 Finite Volume Methods

Although finite difference methods are derived in a natural and simple way, many difficulties arise while working with discontinuous solutions. Rather than approximation of pointwise values, another method was introduced called finite volume methods which produces approximations of the average of the solution in each cell. Let us illustrate the finite volume method for a scalar hyperbolic conservation law [4]. We

recall the Cauchy problem

$$\begin{cases} u_t + f(u)_x = 0, & x \in \mathbb{R}, t \geq 0, \\ u(x,0) = u_0(x). \end{cases} \tag{3.2.1}$$

We define a uniform mesh consisting of cells $C_j = (x_{j-\frac{1}{2}}, x_{j+\frac{1}{2}})$ of fixed length Δx

$$\Delta x = x_{j+\frac{1}{2}} - x_{j-\frac{1}{2}}.$$

Let x_j be the centre of cell C_j:

$$x_j = \frac{1}{2}(x_{j+\frac{1}{2}} + x_{j-\frac{1}{2}}), \quad x_{j+\frac{1}{2}} = x_j + \frac{\Delta x}{2}, \quad j = \ldots, -1, 0, 1, 2, \ldots$$

We also introduce a discretisation in time of fixed time step Δt and discrete time levels t_n

$$t_n = n\Delta t, \qquad n = 0, 1, 2, \ldots$$

The idea of finite volume methods relies on the integral form of the hyperbolic conservation law. Hence we proceed by integrating (3.2.1) over $K_j = C_j \times (t_n, t_{n+1})$

$$\begin{aligned} 0 &= \int_{K_j} \big(u_t + f(u)_x\big) dx dt \\ &= \int_{t_n}^{t_{n+1}} \int_{C_j} \big(u_t + f(u)_x\big) dx dt \\ &= \int_{t_n}^{t_{n+1}} \int_{x_{j-\frac{1}{2}}}^{x_{j+\frac{1}{2}}} u_t dx dt + \int_{t_n}^{t_{n+1}} \int_{x_{j-\frac{1}{2}}}^{x_{j+\frac{1}{2}}} f(u)_x dx dt. \end{aligned}$$

So after integrating by parts, the integral form of (3.2.1) is

$$\int_{x_{j-\frac{1}{2}}}^{x_{j+\frac{1}{2}}} \big(u(x, t_{n+1}) - u(x, t_n)\big) dx + \int_{t_n}^{t_{n+1}} \Big(f(u(x_{j+\frac{1}{2}}, t)) - f(u(x_{j-\frac{1}{2}}, t))\Big) dt = 0. \tag{3.2.2}$$

Dividing by $\Delta t \Delta x$, we obtain:

$$\begin{aligned} 0 =& \frac{1}{\Delta t \Delta x}\left[\int_{x_{j-\frac{1}{2}}}^{x_{j+\frac{1}{2}}} \big(u(x,t_{n+1}) - u(x,t_n)\big)dx + \int_{t_n}^{t_{n+1}} \Big(f(u(x_{j+\frac{1}{2}},t)) - f(u(x_{j-\frac{1}{2}},t))\Big)\,dt\right] \\ &= \frac{1}{\Delta t}\int_{x_{j-\frac{1}{2}}}^{x_{j+\frac{1}{2}}} \frac{1}{\Delta x}\big(u(x,t_{n+1}) - u(x,t_n)\big)dx + \frac{1}{\Delta x}\int_{t_n}^{t_{n+1}} \frac{1}{\Delta t}\Big(f(u(x_{j+\frac{1}{2}},t)) - f(u(x_{j-\frac{1}{2}},t))\Big)\,dt. \end{aligned} \tag{3.2.3}$$

If we define the following cell averages by

$$\begin{aligned} \bar{u}_j^n(x,t) &= \frac{1}{\Delta x}\int_{x_{j-\frac{1}{2}}}^{x_{j+\frac{1}{2}}} u(x,t_n)dx, \\ \bar{f}_{j+\frac{1}{2}}^n &= \frac{1}{\Delta t}\int_{t_n}^{t_{n+1}} f(u(x_{j+\frac{1}{2}},t))dt, \end{aligned} \tag{3.2.4}$$

then, from (3.2.4) and (3.2.3), it follows

$$\frac{1}{\Delta t}[\bar{u}_j^{n+1} - \bar{u}_j^n] + \frac{1}{\Delta x}[\bar{f}_{j+\frac{1}{2}}^n - \bar{f}_{j-\frac{1}{2}}^n] = 0. \tag{3.2.5}$$

As we attempt to derive a method which approximates the cell average of the solution u, the exact relation (3.2.5) suggests the following numerical method

$$\frac{1}{\Delta t}[U_j^{n+1} - U_j^n] + \frac{1}{\Delta x}[F_{j+\frac{1}{2}}^n - F_{j-\frac{1}{2}}^n] = 0, \tag{3.2.6}$$

where U_j^n is the approximation of $\bar{u}_j^n$ and $F_{j+\frac{1}{2}}^n$ is the approximation of $\bar{f}_{j+\frac{1}{2}}^n$, i.e.

$$\begin{aligned} U_j^n &\approx \bar{u}_j^n(x,t), \\ F_{j+\frac{1}{2}}^n &\approx \bar{f}_{j+\frac{1}{2}}^n. \end{aligned} \tag{3.2.7}$$

Considering the natural properties of the problem (3.2.1), we introduce an additional simplification. Due to the hyperbolicity of (3.2.1), which implies finite propagation speed of the information, we can assume that, for small Δt, $F_{j+\frac{1}{2}}^n$ depends only on

the values of the neighbouring cells, i.e.

$$F^n_{j+\frac{1}{2}} = \mathcal{F}(U^n_{j+1}, U^n_j), \tag{3.2.8}$$

where $\mathcal{F}$ is a numerical flux function. Then the method (3.2.6) becomes

$$\frac{1}{\Delta t}[U^{n+1}_j - U^n_j] + \frac{1}{\Delta x}\left[\mathcal{F}(U^n_{j+1}, U^n_j) - \mathcal{F}(U^n_j, U^n_{j-1})\right] = 0 \tag{3.2.9}$$

or

$$U^{n+1}_j = U^n_j - \frac{\Delta t}{\Delta x}\left[\mathcal{F}(U^n_{j+1}, U^n_j) - \mathcal{F}(U^n_j, U^n_{j-1})\right]. \tag{3.2.10}$$

It is concluded that (3.2.10) defines the general form of the finite volume method. Different finite volume methods can be introduced by varying the choice of the numerical flux. A numerical flux is chosen in order to be consistent with the continuous problem (3.2.1), i.e. $\mathcal{F}(u, u) = f(u)$, Lipschitz continuous, monotonically nondecreasing with respect to the first argument and monotonically non-increasing with respect to the second argument (see also section 3.4.1). Consequently, the produced finite volume scheme is conservative.

Definition 3.2.1. A numerical scheme that produces approximations to the solutions of hyperbolic conservation laws is conservative if and only if it mimics the conservation property of the exact solution,i.e. it can be written as

$$u^{n+1}_j = u^n_j - \frac{\Delta t}{\Delta x}[\mathcal{F}(u^n_{j+1}, u^n_j) - \mathcal{F}(u^n_j, u^n_{j-1})], \tag{3.2.11}$$

where $\mathcal{F}$ is Lipschitz continuous and consistent.

Obviously, finite volume schemes preserve the conservation property of the exact solution due to their construction. It is also noticeable that finite volume and finite

difference methods are closed related and we can view a finite volume method as finite difference approximations if we rewrite (3.2.10) as

$$\frac{U_j^{n+1} - U_j^n}{\Delta t} = \frac{\mathcal{F}(U_{j+1}^n, U_j^n) - \mathcal{F}(U_j^n, U_{j-1}^n)}{\Delta x}. \tag{3.2.12}$$

Similarly to finite difference schemes, we conclude that finite volume schemes are stable if the CFL condition (3.1.10) is satisfied.

3.3 Finite Element Method

Before the development of finite volume methods, a completely different approach of producing approximations to solutions of partial differential equations was the finite element method. In comparison with the previous methods, here the approximate solution is defined as a linear combination of piecewise polynomial functions,[6].

Since the finite element method was first introduced, it has found many applications in problems of engineering and mathematical physics and it became very popular. However, the method in its classical form cannot be used for solving hyperbolic conservation laws since its applications leads to nonconservative methods which can be also unstable. For example, in the case of approximating the solution of a hyperbolic conservation law using piecewise linear functions, the finite element method is equivalent to the corresponding central finite difference method which is unstable (see also Appendix A). In order to overcome these issues, one can apply the method on the viscous form of the hyperbolic conservation law, i.e to

$$u_t + f(u)_x = \epsilon u_{xx}, \quad 0 < \epsilon \ll 1, \tag{3.3.1}$$

which now is a parabolic problem and thus the finite element method can be applied very successfully. Recently, a different approach of modifying the classical form of finite element method was introduced to obtain stable schemes for hyperbolic con-

servation laws. The modified form of finite element method is called discontinuous Galerkin method and it is presented later in this chapter.

The idea of finite element method consists of dividing the domain into smaller domains, called elements, and replacing the solution by piecewise approximations produced by a finite set of continuous functions, for example polynomials. The method involves only the weak formulation of the problem. Since the classical finite element method is not suitable for hyperbolic conservation laws, we describe briefly the method for an elliptic problem. We consider the boundary value problem

$$\begin{cases} -u'' = f, & x \in [a,b], \\ u(a) = u(b) = 0, \end{cases} \tag{3.3.2}$$

where $f \in L^2((a,b))$. In order to discretise the problem (3.3.2), we start with deriving its weak formulation. Let $\phi \in H_0^1([a,b])$ be a test function. We multiply (3.3.2) by ϕ, integrate over $[a,b]$ and do integration by parts

$$\int_a^b f\phi dx = -\int_a^b u''\phi dx = \int_a^b u'\phi' dx - u'\phi\Big|_a^b, \qquad \forall \phi \in V.$$

Using the boundary conditions of (3.3.2), we obtain

$$\int_a^b u'\phi' dx = \int_a^b f\phi dx, \qquad \forall \phi \in V. \tag{3.3.3}$$

which is the weak formulation of (3.3.2). Since the finite element framework relies on approximations produced from finite sets of functions, we proceed by introducing a finite dimensional subspace V_h of V. Let $\mathcal{T}$ be a uniform partition of [a,b] consisting

of N subintervals $I_i = [x_i, x_{i+1}]$ of fixed length Δx. Denote

$$\Delta x = \frac{b-a}{N},$$
$$x_i = a + i\Delta x, \quad i = 0, 1, \ldots, N$$

We introduce the finite dimensional space V_h, $dim V_h = N_h$, such that

$$V_h = \{v \in H_0^1([a,b]), v|_{I_i} \in \mathbb{P}^r(I_i)\},$$

where $\mathbb{P}^r$ is the set of polynomials of degree r. Then the finite element method is defined as follows: we seek $u_h \in V_h$ an approximation of u, that satisfies

$$\int_a^b u_h' \phi' dx = \int_a^b f\phi dx, \qquad \forall \phi \in V_h. \tag{3.3.4}$$

Let $\phi_1, \phi_2, \ldots \phi_{N_h}$ be a basis of V_h. Functions $\phi \in \{\phi_i\}_{i=1}^{N_h}$ are called basis functions. Then it follows that we can define u_h as linear combinations of ϕ_j

$$u_h = \sum_{j=1}^{N_h} u_j \phi_j(x), \tag{3.3.5}$$

where the set of coefficients u_j need to be determined. The coefficients u_j are referred as degrees of freedom. In addition, the test function ϕ can be considered as one of the basis functions, i.e. $\phi \in \{\phi_i\}_{i=1}^{N_h}$. Suppose $\phi = \phi_k$, $k = 1, \ldots, N_h$. Then (3.3.4) yields

$$\int_a^b f\phi_k dx = \int_a^b \left[\sum_{j=1}^{N_h} u_j \phi_j'\right] \phi_k' dx = \sum_{j=1}^{N_h} \int_a^b u_j \phi_j' \phi_k' dx.$$

Hence,

$$\sum_{j=1}^{N_h} u_j \int_a^b \phi_j' \phi_k' dx = \int_a^b f\phi_k dx, \qquad k = 1, \ldots, N_h. \tag{3.3.6}$$

or

$$\sum_{j=1}^{N_h} \left[\int_a^b \phi_j' \phi_k' dx \right] u_j = \int_a^b f \phi_k dx, \qquad k = 1, \ldots, N_h. \tag{3.3.7}$$

We observe that (3.3.7) is a linear system and it can be written in a matrix form

$$SU = F, \tag{3.3.8}$$

where S is referred as a stiffness matrix, U the vector of unknowns and F the loading vector. These quantities are defined as follows

$$S = \begin{bmatrix} \int_a^b \phi_1' \phi_1' dx & \cdots & \int_a^b \phi_1' \phi_{N_h}' dx \\ \vdots & \ddots & \vdots \\ \int_a^b \phi_{N_h}' \phi_1' dx & \cdots & \int_a^b \phi_{N_h}' \phi_{N_h}' dx \end{bmatrix}, U = \begin{bmatrix} u_1 \\ \vdots \\ u_{N_h} \end{bmatrix}, F = \begin{bmatrix} \int_a^b f \phi_1 dx \\ \vdots \\ \int_a^b f \phi_{N_h} dx \end{bmatrix} \tag{3.3.9}$$

The matrix S is symmetric and positive definite, resembling the corresponding properties of the Laplace operator of (3.3.2). Thus S is invertible and it yields that the system (3.3.8) has a unique solution U. So the approximate solution u_h is completely determined. In practice, the basis functions $\{\phi_i\}_{i=1}^{N_h}$ are polynomials that have compact support which usually covers few subintervals I_i of the discretisation $\mathcal{T}$. For example, in the case of linear elements, i.e. when $\{\phi_i\}_{i=1}^{N_h}$ are first-degree polynomials, the support is just two subintervals. Consequently, S is a symmetric tridiagonal matrix and the system (3.3.8) can be solved easily. For higher degree of polynomials basis, one can check easily that S is a banded matrix and the number of non-zeros entries depends on the number of subintervals consisting the support of the basis functions. Such systems can be solved by efficient numerical solver which can be either direct, like the Cholesky decomposition, or iterative like the conjugate gradient method.

Accordingly, finite element method can be generalised for nonlinear elliptic as well as for parabolic problems. For approximating solutions to hyperbolic conservation

laws, we introduce a suitable version of the finite element method.

3.4 Discontinuous Galerkin Method

Discontinuous Galerkin method is a special class of finite element methods where the continuity of basis functions across the element is not assumed. The corresponding basis functions are completely discontinuous across each element interface and they usually consist of piecewise polynomials defined locally. Due to the piecewise discontinuous basis functions, the discontinuous Galerkin method can be applied locally in each element. This implies further flexibility, such as having different degrees of freedom in each element independent of their neighbours, which is not allowed in classical finite element method.

The discontinuous Galerkin method was first proposed in 1973 by Reed and Hill [7] and it was designed for solving neutron transport equations, i.e. time-independent linear hyperbolic equations. Later the method has been extended for solving linear and nonlinear time-dependent equations and it has found applications in various areas such as gas dynamics, fluid dynamics and viscoelastic flows.

Let us present first the method for a scalar hyperbolic conservation law.

3.4.1 DG Method for Scalar Hyperbolic Conservation Laws

We consider again the Cauchy problem

$$\begin{cases} u_t + f(u)_x = 0, & x \in [a,b], t \geq 0, \\ u(x,0) = u_0(x), & x \in [a,b]. \end{cases} \tag{3.4.1}$$

Motivated by the finite element framework, we introduce a space discretisation consisting of N cells I_i of length h_i

$$I_i = [x_{i-\frac{1}{2}}, x_{i+\frac{1}{2}}] \qquad \text{and} \qquad h_i = x_{i+\frac{1}{2}} - x_{i-\frac{1}{2}}.$$

We assume that the mesh is regular, i.e there exists a constant $c > 0$ independent of h such that

$$ch \leq h_i,$$

where $h = max_{i\in[1,N]}h_i$. To define the discontinuous Galerkin method we first consider a variational formulation of (3.4.1). Let u be a smooth test function. Then multiplying (3.4.1) by v and integrating over I_i we derive

$$\begin{aligned} 0 &= \int_{I_i} (u_t + f(u)_x)\, v dx \\ &= \int_{I_i} u_t v dx + \int_{I_i} f(u)_x v dx \\ &= \int_{I_i} u_t v dx + f(u)v\Big|_{x_{i-\frac{1}{2}}}^{x_{i+\frac{1}{2}}} - \int_{I_i} f(u)v' dx. \end{aligned}$$

This motivates us to define a finite dimensional space consisting of piecewise polynomials

$$V_h^r = \{v \in L^2([a,b]) : v|_{I_i} \in \mathbb{P}^r(I_i)\},$$

where $\mathbb{P}^r$ is the set of polynomials of degree up to r on I_i. Thus, we seek $u_h \in V_h^r$ an approximate solution of (3.4.1), such that for all test functions $\phi \in V_h^r$ satisfies the following, the semi-discrete discontinuous Galerkin method is defined as follows: find $u_h \in V_h^r$ such that for all elements we have

$$\int_{I_i} (u_h)_t \phi dx = \int_{I_i} f(u_h)\phi' dx - \hat{f}_{i+\frac{1}{2}}\phi(x_{i+\frac{1}{2}}) + \hat{f}_{i-\frac{1}{2}}\phi(x_{i-\frac{1}{2}}), \qquad \forall \phi \in V_h^r, \quad (3.4.2)$$

where $\hat{f}_{i+\frac{1}{2}}$ approximates the boundary terms of the problem (3.4.1) and it is called numerical flux. The way we choose this numerical flux can be considered as the key idea of discontinuous Galerkin method since it merge the classical finite element and the finite volume methods. In general, the numerical flux $\hat{f}_{i+\frac{1}{2}}$ is defined as a two variable function which depends on the value of approximate solution u_h from both

sides of the interface $x_{i+\frac{1}{2}}$, i.e.

$$\hat{f}_{i+\frac{1}{2}} = \hat{f}(u_h(x^-_{i+\frac{1}{2}}, t), u_h(x^+_{i+\frac{1}{2}}, t)),$$

and it has the following properties:

1. Consistency:

   If we evaluate the numerical flux $\hat{f}$ when the solution u is constant across the interface, then it gives the value of f on u,

   $$\hat{f}(u, u) = f(u).$$

2. Lipschitz Continuity:

   The numerical flux $\hat{f}(\cdot, \cdot)$ is at least Lipschitz continuous with respect to both arguments.

3. Monotonicity:

   The numerical flux $\hat{f}(\cdot, \cdot)$ is an increasing function of the first argument and a decreasing function of its second argument.

The consistency and the Lipschitz continuity are required in order to obtain a conservative scheme, while monotonicity ensures that the numerical schemes satisfy all entropy conditions and has the total variation diminishing property (TVD) property, i.e. $TV(U^{n+1}) \leq TV(U^n)$ where $TV(U^n) = \sum_j |U^n_j - U^n_{j-1}|$, [5].
We note that the numerical fluxes for finite difference and finite volume methods also have these properties.

3.4.2 Implementation of the DG method

We provide some details concerning the implementation of the discontinuous Galerkin method. We consider a uniform space discretisation of $N+1$ grid points:

$$a = x_{\frac{1}{2}} < x_{\frac{3}{2}} < \ldots < x_{j-\frac{1}{2}} < x_{j+\frac{1}{2}} < \ldots < x_{\frac{N+1}{2}} = b, \tag{3.4.3}$$

and we define N cells I_i of length Δx by

$$I_i = [x_{i-\frac{1}{2}}, x_{i+\frac{1}{2}}] \qquad \text{and} \qquad \Delta x = x_{i+\frac{1}{2}} - x_{i-i\frac{1}{2}}.$$

We also introduce a discretisation in time of fixed time step Δt and discrete time levels t_n

$$t_n = n\Delta t, \qquad n = 0, 1, 2, \ldots$$

Recall the semi-discrete scheme of the (3.4.1) given by (3.4.2): find $u_h \in V_h^r$ such that

$$\int_{I_i} (u_h)_t \phi dx = \int_{I_i} f(u_h)\phi' dx - \hat{f}_{i+\frac{1}{2}}\phi(x_{i+\frac{1}{2}}) + \hat{f}_{i-\frac{1}{2}}\phi(x_{i-\frac{1}{2}}), \qquad \forall \phi \in V_h^r.$$

In comparison with the classical finite element method, here the basis functions, i.e. the basis of V_h^r, are discontinuous across each element. Common choices of basis function are either the Lagrange polynomials or the Legendre polynomials, whose orthogonality property simplify the computations. Here, we consider the Legendre polynomials up to degree r as the basis functions. In the reference element $[-1, 1]$, the Legendre polynomials are defined recursively as follows:

$$\begin{cases} P_0(x) = 1, P_1(x) = x, \\ mP_n(x) = (2m-1)xP_{m-1}(x) - (m-1)P_{m-2}(x), \qquad \forall m = 2, 3, \ldots \end{cases} \tag{3.4.4}$$

In order to define them in every element $I_i = [x_{i-\frac{1}{2}}, x_{i+\frac{1}{2}}]$, we use the following map

$$x = \frac{x_{i+\frac{1}{2}} - x_{i-\frac{1}{2}}}{2}\xi + \frac{x_{i+\frac{1}{2}} + x_{i-\frac{1}{2}}}{2} = \frac{\Delta x}{2}\xi + \frac{x_{i+\frac{1}{2}} + x_{i-\frac{1}{2}}}{2}, \tag{3.4.5}$$

where $\xi \in [-1, 1]$ and $x \in I_i$. We denote the local Legendre polynomials in I_i by $\tilde{P}_m$, $m = 0, 1, \ldots, r$

$$\tilde{P}_j(x) = \tilde{P}_j(\frac{\Delta x}{2}\xi + \frac{x_{i+\frac{1}{2}} + x_{i-\frac{1}{2}}}{2}).$$

Then, the approximate solution $u_h \in I_i$ can be written as

$$u_h\Big|_{I_i} = \sum_{j=0}^{r} u_j(t)\tilde{P}_j(x), \tag{3.4.6}$$

where the coefficients u_j need to be determined. From (3.4.6), the relation (3.4.2) becomes

$$\int_{I_i}\left[\sum_{j=0}^{r} u_j(t)\tilde{P}_j\right]_t \tilde{P}_l dx = \int_{I_i} f(u_h)\tilde{P}_l' dx - \hat{f}_{i+\frac{1}{2}}\tilde{P}_l(x_{i+\frac{1}{2}}) + \hat{f}_{i-\frac{1}{2}}\tilde{P}_l(x_{i-\frac{1}{2}}), \qquad l = 0, \ldots, r,$$

$$\sum_{j=0}^{r} \dot{u_j}\left[\int_{I_i} \tilde{P}_j\tilde{P}_l dx\right] = \int_{I_i} f(u_h)\tilde{P}_l' dx - \hat{f}_{i+\frac{1}{2}}\tilde{P}_l(x_{i+\frac{1}{2}}) + \hat{f}_{i-\frac{1}{2}}\tilde{P}_l(x_{i-\frac{1}{2}}), \qquad l = 0, \ldots, r,$$

where $\dot{u_j}$ denotes the time derivative. So, for $l = 0, \ldots, r$ we obtain

$$\sum_{j=0}^{r} \dot{u_j}\int_{I_i} \tilde{P}_j\tilde{P}_l dx = \int_{I_i} f(u_h)\tilde{P}_l' dx - \hat{f}_{i+\frac{1}{2}}\tilde{P}_l(x_{i+\frac{1}{2}}) + \hat{f}_{i-\frac{1}{2}}\tilde{P}_l(x_{i-\frac{1}{2}}). \tag{3.4.7}$$

A fully discrete scheme of (3.4.1) can be derived using an approximation of the time derivative $\dot{u_j}$, with the simplest being the forward Euler method

$$u_t(x, t_n)\Big|_{I_i} \approx \frac{U^{n+1} - U^n}{\Delta t}. \tag{3.4.8}$$

Therefore, a fully discrete approximation is defined as follows: find $u_h \in V_h^r$ such that $\forall l$

$$\sum_{j=0}^{r} \frac{U_j^{i,n+1} - U_j^{i,n}}{\Delta t} \int_{I_i} \tilde{P}_j \tilde{P}_l dx = \int_{I_i} f(U^n|_{I_i}) \tilde{P}_l' dx - \hat{f}^n_{i+\frac{1}{2}} \tilde{P}_l(x_{i+\frac{1}{2}}) + \hat{f}^n_{i-\frac{1}{2}} \tilde{P}_l(x_{i-\frac{1}{2}}), \tag{3.4.9}$$

where $\hat{f}^n_{i+\frac{1}{2}} = \mathcal{F}(U^n\big|_{I_{i+1}}, U^n\big|_{I_i})$ and $U^n|_{I_i} = \sum_{j=0}^r U_j^{i,n} \tilde{P}_j$ is the approximate solution on I_i at time level $t_n = n\Delta t$. Rearranging (3.4.9), we get

$$\begin{aligned} \sum_{j=0}^{r} U_j^{i,n+1} \int_{I_i} \tilde{P}_j \tilde{P}_l dx = &\sum_{j=0}^{r} U_j^{i,n} \int_{I_i} \tilde{P}_j \tilde{P}_l dx \\ &+ \Delta t \left[\int_{I_i} f(U^n|_{I_i}) \tilde{P}_l' dx - \hat{f}^n_{i+\frac{1}{2}} \tilde{P}_l(x_{i+\frac{1}{2}}) + \hat{f}^n_{i-\frac{1}{2}} \tilde{P}_l(x_{i-\frac{1}{2}}) \right] \qquad \forall l. \end{aligned} \tag{3.4.10}$$

As with the classical finite element method, (3.4.10) yields to linear system in every element. Therefore for $i = 1, \ldots, N$ we can rewrite (3.4.10) as

$$G^i \mathcal{U}^{i,n+1} = G^i \mathcal{U}^{i,n} + \Delta t \left[S^{i,n} - \hat{f}^n_{i+\frac{1}{2}} B^{i,+} + \hat{f}^n_{i-\frac{1}{2}} B^{i,-} \right], \tag{3.4.11}$$

where G^i is referred as a mass matrix, $S^{i,n}$ the stiffness vector, $\mathcal{U}^{i,n}$ the vector of unknowns and $B^{i,\pm}$ the basis evaluations vector at time step t_n,

$$G^i = \begin{bmatrix} \int_{I_i} \tilde{P}_0 \tilde{P}_0 dx & \cdots & \int_{I_i} \tilde{P}_0 \tilde{P}_r dx \\ \vdots & \ddots & \vdots \\ \int_{I_i} \tilde{P}_r \tilde{P}_0 dx & \cdots & \int_{I_i} \tilde{P}_r \tilde{P}_r dx \end{bmatrix}, \mathcal{U}^{i,n} = \begin{bmatrix} U_1^{i,n} \\ \vdots \\ U_r^{i,n} \end{bmatrix}, S^{i,n} = \begin{bmatrix} \int_{I_i} f(U^n|_{I_i}) \tilde{P}_0' dx \\ \vdots \\ \int_{I_i} f(U^n|_{I_i}) \tilde{P}_r' dx \end{bmatrix},$$

$$B^{i,+} = \left[\tilde{P}_0(x_{i+\frac{1}{2}}), \ldots, \tilde{P}_r(x_{i+\frac{1}{2}}) \right], \qquad B^{i,-} = \left[\tilde{P}_0(x_{i-\frac{1}{2}}), \ldots, \tilde{P}_r(x_{i-\frac{1}{2}}) \right].$$

Considering the definition (3.2), (3.4.11) implies that the discontinuous Galerkin schemes are conservative.

In practice we do not compute the matrix form (3.4.11) on an arbitrary element.

We are interested in computing the matrices in the reference element [-1,1] in order to take advantage of various properties of the basis functions and then transforming them in every element. We map the matrix G^i and vectors $S^{i,n}, B^{i,\pm}$ of an arbitrary element to the reference element. Let's start with the mass matrix G^i in I_i. From (3.4.11) the mass matrix, for $i = 1, \ldots, N$, is given by

$$G^i_{jl} = \int_{I_i} \tilde{P}_j(x)\tilde{P}_l(x)dx, \qquad \forall j, l.$$

Replacing the expression of x given by (3.4.5), we obtain

$$\begin{aligned} G^i_{jl} &= \int_{I_i} \tilde{P}_j(x)\tilde{P}_l(x)dx \\ &= \frac{\Delta x}{2}\int_{-1}^{1} \tilde{P}_j(\frac{\Delta x}{2}\xi + \frac{x_{i+\frac{1}{2}} + x_{i-\frac{1}{2}}}{2})\tilde{P}_l(\frac{\Delta x}{2}\xi + \frac{x_{i+\frac{1}{2}} + x_{i-\frac{1}{2}}}{2})d\xi. \end{aligned} \tag{3.4.12}$$

Considering the actual effect of mapping (3.4.5) onto $\tilde{P}_j$, we realise that (3.4.5) just shifts the domain of function $\tilde{P}_j$ right or left. But the values of $\tilde{P}_j$ are not affected, which yields to the following relation

$$\tilde{P}_j(x) = \tilde{P}_j(\frac{\Delta x}{2}\xi + \frac{x_{i+\frac{1}{2}} + x_{i-\frac{1}{2}}}{2}) = P_j(\xi), \tag{3.4.13}$$

where $\xi \in [-1, 1]$ and $x \in I_i$. Thus, for every element the relation (3.4.12) becomes

$$\begin{aligned} G^i_{jl} &= \frac{\Delta x}{2}\int_{-1}^{1} \tilde{P}_j(\frac{\Delta x}{2}\xi + \frac{x_{i+\frac{1}{2}} + x_{i-\frac{1}{2}}}{2})\tilde{P}_l(\frac{\Delta x}{2}\xi + \frac{x_{i+\frac{1}{2}} + x_{i-\frac{1}{2}}}{2})d\xi \\ &= \frac{\Delta x}{2}\int_{-1}^{1} P_j(\xi)P_l(\xi)d\xi, \qquad \forall j, l. \end{aligned} \tag{3.4.14}$$

Due to orthogonal property of Legendre polynomials with respect to L^2 norm, the

integrals are computed directly as follows

$$\int_{-1}^{1} P_j(y)P_l(y)dy = \frac{2}{2j+1}\delta_{jl} = \begin{cases} 0 & , \quad \text{if } j \neq l, \\ \dfrac{2}{2j+1} & , \quad \text{if } j = l. \end{cases} \tag{3.4.15}$$

Thus, the mass matrix G^i becomes diagonal. In case of uniform grids, the mass matrix G^i is the same for all elements and all time steps. In general, if the basis functions are not orthogonal, the integral will be computed using the Gauss-Legendre quadrature rule. In case of polynomial functions, an integral can be computed exactly. According to Gauss-Legendre quadrature rule

$$\int_{-1}^{1} p(\xi)d\xi \approx \sum_{q=1}^{r+1} w_q p(\xi_q), \tag{3.4.16}$$

where ξ_q are the Gauss-Legendre points and w_q the corresponding weights. If p are polynomials of degree r, (3.4.16) is exact if we use $\frac{r+1}{2}$ Gauss-Legendre points. Similarly, we seek the mapping of the stiffness vector from an arbitrary element to the reference element. From (3.4.11) and (3.4.5), for all i, we obtain

$$\begin{aligned} S^{i,n} &= \int_{I_i} f(U^n|_{I_i})\tilde{P}_l'(x)dx \\ &= \frac{\Delta x}{2}\int_{-1}^{1} f(U^n|_{I_i})\tilde{P}_l'(\frac{\Delta x}{2}\xi + \frac{x_{i+\frac{1}{2}} + x_{i-\frac{1}{2}}}{2})\frac{2}{\Delta x}d\xi, \qquad l = 0, .., r. \end{aligned}$$

So, from observation (3.4.13), the stiffness vector $S^{i,n}$ becomes

$$S_l^{i,n} = \int_{-1}^{1} f(U^n|_{I_i}^{\xi})P_l'(\xi)d\xi, \qquad l = 0, .., r,$$

where

$$U^n\big|_{I_i} = \sum_{j=0}^{r} U_j^n \tilde{P}_j(x), \qquad U^n\big|_{I_i}^{\xi} = \sum_{j=0}^{r} U_j^n P_j(\xi),$$

and

$$U^n|_{I_i} = U^n|_{I_i}^{\xi} . \tag{3.4.17}$$

Here, the integrals are computed using the Gauss-Legendre quadrature rule. Due to the nonlinearity of $f(u)$, the quadrature rule produces approximation to the integrals. Hence, for $l = 0, .., r$

$$S_l^{i,n} = \int_{-1}^{1} f(U^n|_{I_i}^{\xi}) P_l'(\xi) d\xi \approx \sum_{q=1}^{r+1} w_q f(U^n|_{I_I}^{\xi_q}) P_l'(\xi_q).$$

In comparison with the mass matrix G^i, the stiffness vector $S^{i,n}$ is not the same for all elements and all time steps. Because of its components involve the approximate solution $U^{i,n}\big|_{I_i}$ which changes in space and time, $S^{i,n}$ is uniquely determined for each element at every time level.

At this point, it should be mentioned that the observation (3.4.13) can be applied on evaluating the approximate solution u_h on a random point in I_i. From (3.4.6), we can conclude easily that

$$\begin{aligned} u_h\Big|_{I_i} &= \sum_{j=0}^{r} U_j^n \tilde{P}_j(x) = \sum_{j=0}^{r} U_j^n \tilde{P}_j(\frac{\Delta x}{2}\xi + \frac{x_{i+\frac{1}{2}} + x_{i-\frac{1}{2}}}{2}) \\ &= \sum_{j=0}^{r} U_j^n P_j(\xi), \qquad \xi \in [-1, 1], x \in I_i, n = 0, 1, \dots \end{aligned} \tag{3.4.18}$$

Finally, due to (3.4.13), the mapping of basis evaluations vectors from an arbitrary element I_i to the reference element becomes trivial. From (3.4.11) and (3.4.5), for every element it follows that

$$B^{i,+} = \Big[P_0(1), \dots, P_r(1)\Big], \qquad B^{i,-} = \Big[P_0(-1), \dots, P_r(-1)\Big] .$$

Considering the property of Legendre polynomials,

$$P_m(1) = 1, \qquad P_m(-1) = (-1)^m, \qquad \forall m,$$

then we obtain the constant basis evaluations vectors

$$B^{i,+} = \left[1, 1, \ldots, 1\right], \qquad B^{i,-} = \left[1, -1, \ldots, (-1)^{r-1}, (-1)^r\right].$$

Consequently, after all manipulations, the system (3.4.11) $\forall i$ is given as

$$G^i \mathcal{U}^{i,n+1} = G^i \mathcal{U}^{i,n} + \Delta t \left[S^{i,n} - \hat{f}^n_{i+\frac{1}{2}} B^{i,+} + \hat{f}^n_{i-\frac{1}{2}} B^{i,-}\right], \tag{3.4.19}$$

where the matrix G^i and the vectors $S^{i,n}, U^{i,n}, B^{i,+}$ and $B^{i,-}$ are simplified as follows

$$G^i = \frac{\Delta x}{2} \begin{bmatrix} 2 & 0 & \cdots & 0 \\ 0 & \frac{2}{3} & \cdots & 0 \\ \vdots & \vdots & \ddots & \vdots \\ 0 & 0 & \cdots & \frac{2}{2r+1} \end{bmatrix}, \mathcal{U}^{i,n} = \begin{bmatrix} U_1^{i,n} \\ \vdots \\ U_r^{i,n} \end{bmatrix}, S^{i,n} = \begin{bmatrix} \sum_{q=1}^{r+1} w_q f(U^n|_{I_I}^{\xi_q}) P_0'(\xi_q) \\ \vdots \\ \sum_{q=1}^{r+1} w_q f(U^n|_{I_I}^{\xi_q}) P_r'(\xi_q) \end{bmatrix},$$

$$B^{i,+} = \left[1, 1, \ldots, 1\right], \qquad B^{i,-} = \left[1, -1, \ldots, (-1)^{r-1}, (-1)^r\right].$$

Now, all required items for the implementation are constructed and the system (3.4.19) for every element is represented in terms of the to reference element. We note that the solution is computed locally in every element and thus the solution of a large systems is avoided.

3.4.3 DG Method for Systems of Hyperbolic Conservation Laws

The discontinuous Galerkin method can be extended straightforwardly to the case of systems. The key idea of this generalisation is to apply the method component-wise and choose numerical fluxes that involve all the unknown variables. In this section, to facilitate the presentation, we describe the method for a quasilinear system consisting of two scalar hyperbolic conservation laws. We consider the system

$$u_t + f(v)_x = 0, \qquad x \in [a,b], \qquad t \geq 0, \tag{3.4.20a}$$

$$v_t + g(u)_x = 0. \tag{3.4.20b}$$

As before, we introduce a space discretisation consisting of cells I_i of length Δx by

$$I_i = [x_{i-\frac{1}{2}}, x_{i+\frac{1}{2}}] \qquad \text{and} \qquad \Delta x = x_{i+\frac{1}{2}} - x_{i-\frac{1}{2}}.$$

We define the finite element space $V_h^r = \{v \in L^2([a,b]) : v|_{I_i} \in P^r(I_i)\}$ and let $u_h, v_h \in V_h^r$ be the approximations to u and v respectively. As in the case of scalar hyperbolic conservation laws, we derive a semi-discrete form of each equation of the system. Let $\phi \in V_h^r$ be a test function. Then, from (3.4.20a) we obtain

$$\begin{aligned} 0 &= \int_{I_i} \Big[(u_h)_t + f(v_h)_x\Big]\phi dx \\ &= \int_{I_i} (u_h)_t \phi dx + \int_{I_i} f(v_h)_x \phi dx \\ &= \int_{I_i} (u_h)_t \phi dx - \int_{I_i} f(v_h)\phi' dx + f(v_h)\phi\Big|_{I_i}, \qquad \forall \phi \in V_h^r. \end{aligned}$$

Similarly, from (3.4.20b) we obtain

$$\int_{I_i} (v_h)_t \phi dx - \int_{I_i} g(u_h)\phi' dx + g(u_h)\phi\Big|_{I_i} = 0, \qquad \forall \phi \in V_h^r.$$

Then the semi-discrete discontinuous Galerkin method of (3.4.20) is defined by: we seek $u_h, v_h \in V_h^r$ approximations to u and v respectively such that for all test function $\phi \in V_h^r$ satisfy the following

$$\begin{cases} \int_{I_i} (u_h)_t \phi dx = \int_{I_i} f(v_h)\phi' dx - \hat{f}_{i+\frac{1}{2}}\phi(x_{i+\frac{1}{2}}) + \hat{f}_{i-\frac{1}{2}}\phi(x_{i-\frac{1}{2}}), \\ \int_{I_i} (v_h)_t \phi dx = \int_{I_i} g(u_h)\phi' dx - \hat{g}_{i+\frac{1}{2}}\phi(x_{i+\frac{1}{2}}) + \hat{g}_{i-\frac{1}{2}}\phi(x_{i-\frac{1}{2}}), \end{cases} \tag{3.4.21}$$

where $\hat{f}_{i+\frac{1}{2}} = \mathcal{F}(u^+_{i+\frac{1}{2}}, u^-_{i+\frac{1}{2}}, v^+_{i+\frac{1}{2}}, v^-_{i+\frac{1}{2}})$ and $\hat{g}_{i+\frac{1}{2}} = \mathcal{G}(u^+_{i+\frac{1}{2}}, u^-_{i+\frac{1}{2}}, v^+_{i+\frac{1}{2}}, v^-_{i+\frac{1}{2}})$ are the numerical fluxes. The numerical fluxes $\mathcal{F}$ and $\mathcal{G}$ are not necessarily same but they should satisfy the properties referred on the numerical flux at the scalar case, i.e. consistency, Lipschitz continuity and monotonicity to obtain the conservation property of the scheme (see also section 3.4.1).

Remark 3.4.1. A numerical flux used for the scalar case can be generalised to the case of systems. In order to obtain the generalised form of the flux, it is reasonable to rewrite the system (3.4.20) in a compact form in respect of the scalar equation. Hence, the system (3.4.20) can be rewritten as follows

$$U_t + A(U)U_x = 0, \tag{3.4.22}$$

where A $\in \mathbb{R}^{2\times 2}$ is a matrix depending on U, where $U : \mathbb{R} \times \mathbb{R}_+ \to \mathbb{R}^2$ is the vector of the unknown variables,

$$A = \begin{bmatrix} 0 & f'(v) \\ g'(u) & 0 \end{bmatrix} \qquad \text{and} \qquad U = \begin{bmatrix} u \\ v \end{bmatrix}.$$

Suppose the numerical flux $\hat{f}_{i+\frac{1}{2}}$ in scalar case is

$$\hat{f}_{i+\frac{1}{2}} = \hat{f}(u^-, u^+), \tag{3.4.23}$$

where $u^- = u_h(x^-_{i+\frac{1}{2}}, t)$ and $u^+ = u_h(x_{i+\frac{1}{2}}{}^+, t)$ are the values of the approximate solution on the left and right element respectively, where the point $x_{i+\frac{1}{2}}$ belongs. Then, the generalised form of the numerical flux is obtained by plugging the expression of U into (3.4.23)

$$\hat{f}_{i+\frac{1}{2}} = \hat{f}(U^+, U^-) = \mathcal{F}(u^+, u^-, v^+, v^-). \tag{3.4.24}$$

Following the procedure of the scalar case, we define similarly the basis functions of V_h^r. We consider the Legendre polynomials up to degree r as the basis functions. It follows that the approximate solutions $u_h, v_h \in I_i$ can be written as

$$u_h\Big|_{I_i} = \sum_{j=0}^{r} u_j(t)\tilde{P}_j(x) \qquad \text{and} \qquad v_h\Big|_{I_i} = \sum_{k=0}^{r} v_k(t)\tilde{P}_k(x). \tag{3.4.25}$$

Then, (3.4.21) yields for $l = 0, \ldots, r$

$$\begin{cases} \displaystyle\int_{I_i} \left[\sum_{j=0}^{r} u_j(t)\tilde{P}_j\right]_t \tilde{P}_l dx = \int_{I_i} f(v_h)\tilde{P}_l' dx - \hat{f}_{i+\frac{1}{2}}\tilde{P}_l(x_{i+\frac{1}{2}}) + \hat{f}_{i-\frac{1}{2}}\tilde{P}_l(x_{i-\frac{1}{2}}), \\ \displaystyle\int_{I_i} \left[\sum_{k=0}^{r} v_k(t)\tilde{P}_k\right]_t \tilde{P}_l dx = \int_{I_i} g(u_h)\tilde{P}_l' dx - \hat{g}_{i+\frac{1}{2}}\tilde{P}_l(x_{i+\frac{1}{2}}) + \hat{g}_{i-\frac{1}{2}}\tilde{P}_l(x_{i-\frac{1}{2}}), \end{cases}$$

or

$$\begin{cases} \displaystyle\sum_{j=0}^{r} \dot{u_j} \int_{I_i} \tilde{P}_j\tilde{P}_l dx = \int_{I_i} f(v_h)\tilde{P}_l' dx - \hat{f}_{i+\frac{1}{2}}\tilde{P}_l(x_{i+\frac{1}{2}}) + \hat{f}_{i-\frac{1}{2}}\tilde{P}_l(x_{i-\frac{1}{2}}), \\ \displaystyle\sum_{k=0}^{r} \dot{v_k} \int_{I_i} \tilde{P}_k\tilde{P}_l dx = \int_{I_i} g(u_h)\tilde{P}_l' dx - \hat{g}_{i+\frac{1}{2}}\tilde{P}_l(x_{i+\frac{1}{2}}) + \hat{g}_{i-\frac{1}{2}}\tilde{P}_l(x_{i-\frac{1}{2}}). \end{cases}$$

Therefore, for $j, k, l = 0, \ldots, r$ we obtain

$$\begin{cases} \displaystyle\sum_{j=0}^{r} \dot{u_j} \int_{I_i} \tilde{P}_j\tilde{P}_l dx = \int_{I_i} f(v_h)\tilde{P}_l' dx - \hat{f}_{i+\frac{1}{2}}\tilde{P}_l(x_{i+\frac{1}{2}}) + \hat{f}_{i-\frac{1}{2}}\tilde{P}_l(x_{i-\frac{1}{2}}), \\ \displaystyle\sum_{k=0}^{r} \dot{v_k} \int_{I_i} \tilde{P}_k\tilde{P}_l dx = \int_{I_i} g(u_h)\tilde{P}_l' dx - \hat{g}_{i+\frac{1}{2}}\tilde{P}_l(x_{i+\frac{1}{2}}) + \hat{g}_{i-\frac{1}{2}}\tilde{P}_l(x_{i-\frac{1}{2}}). \end{cases} \tag{3.4.26}$$

In order to approximate the time derivatives, we recall the forward Euler method

(3.4.8). Then, for $j,k,l=0,\ldots,r$, it follows

$$\begin{cases} \displaystyle\sum_{j=0}^{r} \frac{U_j^{n+1}-U_j^n}{\Delta t}\int_{I_i}\tilde{P}_j\tilde{P}_l dx = \int_{I_i} f(V^n|_{I_i})\tilde{P}_l' dx - \hat{f}^n_{i+\frac{1}{2}}\tilde{P}_l(x_{i+\frac{1}{2}}) + \hat{f}^n_{i-\frac{1}{2}}\tilde{P}_l(x_{i-\frac{1}{2}}), \\ \displaystyle\sum_{k=0}^{r} \frac{V_k^{n+1}-V_k^n}{\Delta t}\int_{I_i}\tilde{P}_k\tilde{P}_l dx = \int_{I_i} g(U^n|_{I_i})\tilde{P}_l' dx - \hat{g}^n_{i+\frac{1}{2}}\tilde{P}_l(x_{i+\frac{1}{2}}) + \hat{g}^n_{i-\frac{1}{2}}\tilde{P}_l(x_{i-\frac{1}{2}}), \end{cases} \tag{3.4.27}$$

where $U^n|_{I_i}=\sum_{j=0}^r U_j^n\tilde{P}_j$ is the approximation to u and $V^n|_{I_i}=\sum_{k=0}^r V_k^n\tilde{P}_k$ is the approximation to v in I_i element at time level $t_n=n\Delta t$. Rearranging (3.4.27), we get

$$\begin{cases} \displaystyle\sum_{j=0}^{r} U_j^{n+1}\int_{I_i}\tilde{P}_j\tilde{P}_l dx = \sum_{j=0}^{r} U_j^n\int_{I_i}\tilde{P}_j\tilde{P}_l dx \\ \qquad\qquad + \Delta t\Big[\displaystyle\int_{I_i} f(V^n|_{I_i})\tilde{P}_l' dx - \hat{f}^n_{i+\frac{1}{2}}\tilde{P}_l(x_{i+\frac{1}{2}}) + \hat{f}^n_{i-\frac{1}{2}}\tilde{P}_l(x_{i-\frac{1}{2}})\Big], \\ \displaystyle\sum_{k=0}^{r} V_k^{n+1}\int_{I_i}\tilde{P}_k\tilde{P}_l dx = \sum_{k=0}^{r} V_k^n\int_{I_i}\tilde{P}_j\tilde{P}_l dx \\ \qquad\qquad + \Delta t\Big[\displaystyle\int_{I_i} g(U^n|_{I_i})\tilde{P}_l' dx - \hat{g}^n_{i+\frac{1}{2}}\tilde{P}_l(x_{i+\frac{1}{2}}) + \hat{g}^n_{i-\frac{1}{2}}\tilde{P}_l(x_{i-\frac{1}{2}})\Big]. \end{cases} \tag{3.4.28}$$

Thus, the linear systems can be rewritten in matrix form as follows

$$\begin{cases} G^i U_j^{i,n+1} = G^i U_j^{i,n} + \Delta t\big[(S_v)^{i,n} - \hat{f}^n_{i+\frac{1}{2}}B^{i,+} + \hat{f}^n_{i-\frac{1}{2}}B^{i,-}\big], \\ G^i V_k^{i,n+1} = G^i V_k^{i,n} + \Delta t\big[(S_u)^{i,n} - \hat{g}^n_{i+\frac{1}{2}}B^{i,+} + \hat{g}^n_{i-\frac{1}{2}}B^{i,-}\big], \end{cases} \tag{3.4.29}$$

for every element $I_i, i=1\ldots,N$. It is noticeable that (3.4.29) consists of two linear systems which are solved explicitly for each time step. Following the simplifications provided for the scalar case, solutions of (3.4.29) can be computed easily.

Chapter 4

Numerical Experiments

In this chapter we present some important results about the error estimation and the stability of discontinuous Galerkin method. Moreover, we illustrate some applications of discontinuous Galerkin scheme to one-dimensional hyperbolic conservation laws. We also compare the approximation to the solution produced by a finite volume scheme and a discontinuous Galerkin scheme. The two methods are applied to the linear advection equation with either smooth or discontinuous initial conditions, to the nonlinear Burgers' equation and a system of elastodynamics.

4.1 Error Estimates and Superconvergence

In order to examine the accuracy of a method, we measure the error, i.e. the difference between the exact and the approximation to the solution. Since the discontinuous Galerkin method is a subclass of finite element methods, we are capable to obtain an a-priori estimation of the error. The following result are included in [24] and [25].

Proposition 4.1.1. Let u be the exact solution of (3.4.1), u smooth, and u_h be the approximation of u computed using the discontinuous Galerkin method. Suppose that the basis functions consist of piecewise polynomials up to degree r. Then the following L^2 error estimate holds

$$\|u - u_h\|_{L^2} \leq Ch^{r+1}, \tag{4.1.1}$$

where h is the length of the elements and C depends on u and its derivatives but is

independent of h.

Furthermore, the error analysis in finite element method usually involves the estimation of the error between the approximate solution and a projection $\mathbb{P}u$ of u into the finite element space V_h^r. The discontinuous Galerkin solution u_h shows a special super-convergent behaviour regarding a Gauss - Radau projection of u. Such projection can be defined either as

$$\int_{I_i} (\mathbb{P}_- u)\ v\ dx = \int_{I_i} u\ v\ dx,\ \forall v \in P^{r-1}(I_i), \qquad \text{and} \qquad \mathbb{P}_- u(x^-_{i+\frac{1}{2}}) = u(x^-_{i+\frac{1}{2}}), \tag{4.1.2}$$

or

$$\int_{I_i} (\mathbb{P}_+ u)\ v\ dx = \int_{I_i} u\ v\ dx,\ \forall v \in P^{r-1}(I_i), \qquad \text{and} \qquad \mathbb{P}_+ u(x^+_{i-\frac{1}{2}}) = u(x^+_{i-\frac{1}{2}}). \tag{4.1.3}$$

The following result, given in [26], describes this super-convergent behaviour of u_h.

Proposition 4.1.2. Let u be the exact solution of (3.4.1), u smooth, and u_h be the approximation of u computed using the discontinuous Galerkin method. Suppose that the basis functions consist of piecewise polynomials up to degree r. Then

$$\|\mathbb{P}u - u_h\|_{L^2} \leq Ch^{r+1+\alpha}, \tag{4.1.4}$$

where h is the mesh size, $\alpha > 0$ the rate of super-convergence and $\mathbb{P}u$ is a Gauss-Radau projection of u into the finite element space V_h^r. For one-dimensional linear hyperbolic conservation laws with uniform meshes, $\alpha = \frac{1}{2}$.

A consequence of this super-convergence is that the constant C in proposition (4.1.1) grows linearly with time, which implies that the error $\|u - u_h\|_{L^2}$ does not grow for time after $t = \frac{1}{\sqrt{h}}$,[26].

4.2 Stability

Stability is considered as one of the most important properties of numerical methods. Roughly speaking, stability guarantees that small perturbations on the initial data does not change the result of the method. In fact, stability implies that for an accurate method, i.e. with small error, the numerical solution converges to the exact solution of the problem. In order to obtain stability of the discontinuous Galerkin scheme described in the previous chapter, we review the CFL condition and we introduce the the concept of limiting. Also, we present the L^2-stability of the approximation to the solution produced by the discontinuous Galerkin scheme.

4.2.1 L^2-Stability

As we have already seen, weak solutions are not necessarily unique and thus the entropy condition is imposed to obtain the physical relevant solution. Let u be the entropy solution of (3.4.1). Then in distribution sense the following entropy inequality is satisfied:

$$U(u)_t + F(u)_x \leq 0, \tag{4.2.1}$$

where U can be any convex entropy function and $F(u) = \int U'(u)f'(u)du$ the corresponding entropy flux. Considering now u_h the discrete approximation to u, we check if u_h satisfies a discrete form of the entropy inequality. From [27], we have the following result.

Proposition 4.2.1. Let u_h be the approximation of u computed using the discontinuous Galerkin method (3.4.2). Then u_h satisfies the following cell entropy inequality:

$$\frac{d}{dt}\int_{I_i} \frac{{u_h}^2}{2}dx + \hat{F}_{i+\frac{1}{2}} - \hat{F}_{i-\frac{1}{2}} \leq 0, \tag{4.2.2}$$

where $\hat{F}_{i+\frac{1}{2}} = \hat{F}(u_h(x^+_{i+\frac{1}{2}}, t), u_h(x^-_{i+\frac{1}{2}}, t))$ is some consistent entropy flux. (Consistency

is defined same as for numerical fluxes, see section 3.4.1).

An immediate consequence of this is the L^2-stability of the approximate solution u_h, see [24].

Proposition 4.2.2. Consider the problem (3.4.1) with some periodic boundary conditions or boundary conditions with compact support . Let u_h be the approximation to the solution using the discontinuous Galerkin method (3.4.2). Then u_h satisfies the following:

$$\frac{d}{dt}\int_0^1 {u_h}^2\, dx \leq 0, \tag{4.2.3}$$

or

$$\|u_h(\cdot,t)\|_{L^2} \leq \|u_h(\cdot,0)\|_{L^2}. \tag{4.2.4}$$

Although the cell entropy and the L^2-stability holds even for discontinuous solutions, they cannot ensure stability of a numerical method. We introduce additional concepts to continue the stability analysis.

4.2.2 CFL condition for DG Method

In section 3.1.1, the CFL condition is defined as a necessary but not sufficient condition to obtain stability of a numerical scheme. For hyperbolic conservation laws, the CFL condition is considered as:

$$\lambda\frac{\Delta t}{\Delta x} \leq 1, \tag{4.2.5}$$

where $\lambda = \max_u |f'(u)|$. Therefore a discontinuous Galerkin scheme (3.4.2) is stable if the above condition is satisfied. Moreover, for discontinuous Galerkin schemes, there exists a special result about CFL condition, see [11].

Lemma 4.2.1. Consider the problem (3.4.1) and the corresponding semi-discrete scheme for the discontinuous Galerkin method (3.4.2). The scheme (3.4.2) is linearly stable

under the CFL condition

$$\max_u |f'(u)| \frac{\Delta t}{\Delta x} \leq \frac{1}{2k+1}, \qquad \text{for } k = 1, 2. \tag{4.2.6}$$

It is noticeable if the ratio $\frac{\Delta t}{\Delta x}$ is constant then the method is unstable. In this case, the scheme (3.4.10) with forward Euler time-discretisation can be stable for polynomial of degree $r = 1$ if the time step Δt is order of $(\Delta x)^{3/2}$, [9].

4.2.3 Limiting

The scheme (3.4.10) is stable only under condition which is strict as mentioned above and for linear problems, it is unconditionally unstable [9]. Consequently, a limiting procedure was introduced to overcome this problem. The idea of limiting procedure was to modify the coefficients of the expansion of the approximate solution in order to produce limiters for the variation of slopes of the solutions. The initial limiting procedure, motivated by the fact that piecewise-constant approximations obtain monotone schemes, introduced a generalised slope limiter to impose the sign property of monotone schemes. Thus the approximate solutions became local projections of themselves into the space of piecewise-linear functions and a weaker CFL condition was required for stability [10], [28]. However, this procedure reduced the accuracy of the solution over the whole domain. Later on, in order to keep the accuracy on smooth regions unaffected, a modification was proposed to the initial procedure [13]. The modified version is based on applying the minmod limiters successively to lower order coefficients and it is explained in the next paragraph. A complete description of minmod limiter procedure is presented in [14].

Let us explained briefly the method. We consider u_h an approximate solution

produced by the discontinuous Galerkin scheme (3.4.10). From (3.4.18), we have

$$u_h\Big|_{I_i} = \sum_{k=0}^{r} U_k^i \tilde{P}_k(x). \tag{4.2.7}$$

We define the minmod function

$$minmod(a,b,c) = \begin{cases} \min(a,b,c), & if sgn(a) = sgn(b) = sgn(c), \\ 0, & otherwise \end{cases} \tag{4.2.8}$$

Thus, the limiter to the coefficients of u_h is defined as

$$(2k+1)U_{k+1}^i = minmod((2k+1)U_{k+1}^i, \Delta U_k^i, \nabla U_k^i), \tag{4.2.9}$$

where ΔU_k^i are the coefficients of $\Delta\bar{u}|_{I_i} = u_h|_{I_{i+1}}(x_{i+\frac{1}{2}},t) - u_h|_{I_i}(x_{i+\frac{1}{2}},t)$ and ∇U_k^i are the coefficients $\nabla\bar{u}|_{I_i} = u_h|_{I_i}(x_{i+\frac{1}{2}},t) - u_h|_{I_{i-1}}(x_{i+\frac{1}{2}},t)$. The limiter is applied starting from the highest order coefficient and is repeated successively to the lowest order coefficients. This process finishes when the first coefficient does not change after the limiting.

4.3 Numerical tests

In this section we exhibit applications of discontinuous Galerkin method to one-dimensional hyperbolic conservation laws. We compare the behaviour of a discontinuous Galerkin scheme with the corresponding finite volume scheme. We illustrate the results for a linear transport equation, a Burgers' equation and the system of elastodynamics. In the following examples, we use the Lax-Friedrichs numerical flux which defined as follows

$$\hat{f}^{LF}(u^+,u^-) = \frac{1}{2}\left(f(u^+) + f(u^-))\right) - \frac{1}{2}\alpha\left(u^+ + u^-\right), \tag{4.3.1}$$

where $\alpha = \max_u |f'(u)|$, $u^+ = u_h(x^+_{j+\frac{1}{2}}, t)$ and $u^+ = u_h(x^-_{j+\frac{1}{2}}, t)$. In particular, we use the local Lax-Friedrichs method

$$\hat{f}^{LLF}(u^+, u^-) = \frac{1}{2}\left(f(u^+) + f(u^-))\right) - \frac{1}{2}\alpha_{j+\frac{1}{2}}\left(u^+ + u^-\right), \tag{4.3.2}$$

where $\alpha_{j+\frac{1}{2}} = \max_{(u^+,u^-)} |f'(u)|$. It can be shown that both forms of Lax-Friedrichs flux satisfy the properties of consistence, Lipschitz continuity and monotonicity, (see section 3.4.1).

Before applying the method to the examples, an important remark about the time discretisation of discontinuous Galerkin schemes is in order. Although the forward Euler method is formed very easily, it is rarely used in practice for discontinuous Galerkin schemes due to stability issues. In practice, the time discretisation of a discontinuous Galerkin scheme involves the Runge-Kutta methods. The Runge-Kutta methods are multistage methods that compute approximations to the solution at intermediate time levels which later combined to advance the solution at the next time level. For a complete presentation on the method, we refer to [10] and [28]. Let us describe the Runge-Kutta discontinuous Galerkin method for a scalar conservation law.

Runge - Kutta time discretisation: We recall the Cauchy problem (3.4.1) and its semi-discrete discontinuous Galerkin scheme (3.4.7). Then, for $l = 0, \ldots, r$ we have

$$\sum_{j=0}^{r} \dot{u_j} \int_{I_i} \tilde{P}_j \tilde{P}_l \ dx = \int_{I_i} f(u_h)\tilde{P}_l' \, dx - \hat{f}_{i+\frac{1}{2}}\tilde{P}_l(x_{i+\frac{1}{2}}) + \hat{f}_{i-\frac{1}{2}}\tilde{P}_l(x_{i-\frac{1}{2}}). \tag{4.3.3}$$

For simplification of the presentation, we denote the right hand side of the above relation as follows

$$\mathcal{L}_l\left(u_h^{(i)}\right) = \int_{I_i} f(u_h)\tilde{P}_l' \ dx - \hat{f}_{i+\frac{1}{2}}\tilde{P}_l(x_{i+\frac{1}{2}}) + \hat{f}_{i-\frac{1}{2}}\tilde{P}_l(x_{i-\frac{1}{2}}). \tag{4.3.4}$$

Hence, the relation (4.3.3) is rewritten as

$$\sum_{j=0}^{r} \dot{u_j} \int_{I_i} \tilde{P}_j \tilde{P}_l \, dx = \mathcal{L}_l \left(u_h^{(i)} \right), \qquad \forall l.$$

In matrix form, the linear system (4.3.3) becomes

$$G^i \dot{U^i} = \mathcal{L} \left(u_h^{(i)} \right), \tag{4.3.5}$$

where the matrix G^i is the mass matrix. Motivated by (4.3.5), the Runge-Kutta discontinuous Galerkin method for (3.4.1) is obtained by discretising the time using the following Runge-Kutta method:

1. Set $U^{i,0} = u_h^n|_{I_i}$, where $u_h^n|_{I_i}$ is the approximate solution at time level n in I_i.

2. Compute the $\mathcal{K}$ intermediate time levels for $m = 1, \ldots, \mathcal{K}$

$$G^i U^{i,m} = \sum_{s=0}^{m-1} \alpha_{m,s} G^i U^{i,s} + \Delta t \beta_{m,s} \mathcal{L} \left(U^{i,s} \right). \tag{4.3.6}$$

   where the coefficients $\alpha_{m,s}$ are non-negative constants with total sum equal to 1 and $\beta_{m,s}$ are constants such that for non-zero $\beta_{m,s}$ it follows that $\alpha_{m,s}$ are also non-zero.

3. Set $u_h^{n+1}\big|_{I_i} = G^i U^{i,\mathcal{K}}$ the solution at the next time level.

This procedure is repeated locally for every element for each time level to produce the approximation to the solution of (3.4.1). A simple example of the method is the two-stage Runge-Kutta method which forms as follows

$$\begin{aligned} G^i U^{i,1} &= G^i U^{i,0} + \Delta t \mathcal{L} \left(U^{i,0} \right), \\ G^i U^{i,n+1} &= \frac{1}{2} G^i U^{i,0} + \frac{1}{2} G^i U^{i,1} + \Delta t \mathcal{L} \left(U^{i,1} \right), \end{aligned} \tag{4.3.7}$$

where $U^{i,0} = u_h|_{I_i}{}^n$. The method (4.3.7) is second order accurate, and thus more accurate than an Euler method which is first order. However, the intermediate time levels of (4.3.7) are forward Euler steps and since the Euler method is unstable [9], the limiting procedure should be applied to obtain stability. For the following examples we use this 2-stage Runge-Kutta discontinuous Galerkin scheme.

4.3.1 Linear transport equation

A transport equation describes the propagation of a variable quantity u along a wave travelling with constant speed α. If $\alpha = 1$, we consider the following problem

$$\begin{cases} u_t + u_x = 0, & x \in [0,1], t \geq 0, \\ u(x,0) = u_0(x), & x \in [0,1], \end{cases} \tag{4.3.8}$$

and the exact solution of (4.3.8) can be computed by the method of characteristics as

$$u(x,t) = u_0(x-t).$$

- Smooth initial condition:

  Considering the problem (4.3.8), we choose the initial condition $u_0(x)$ to be a smooth and periodic function

  $$u_0(x) = sin(2\pi x), \qquad x \in [0,1]. \tag{4.3.9}$$

  Therefore, the exact solution is

  $$u(x,t) = sin(2\pi(x-t)), \qquad x \in [0,1], t \geq 0. \tag{4.3.10}$$

  Let us implement the finite volume scheme (3.2.10) and Runge-Kutta discon-

tinuous Galerkin scheme (4.3.7) to check if they produce reasonable approximations to the solution of (4.3.8). We introduce a uniform mesh consisting of 80 cells I_i and a fixed time step of $\Delta t = 10^{-4}$. Since the choices of space and time steps affect the stability of the schemes, we check if the CFL condition is satisfied. From section 4.2.2, indeed the CFL condition is satisfied

$$\frac{\Delta t}{\Delta x} = \frac{10^{-4}}{0.0125} = 0.008 \leq \frac{1}{2k+1}, \qquad \text{for } k = 1, 2,$$

and thus the scheme (4.3.7) is stable and convergent. Using periodic boundary conditions, i.e $u(0,t) = u(1,t)$, the graph 4.1 demonstrates the exact solution of (4.3.8) at $T = 4.0$ as well as the approximation to the solution produced by the two schemes. It is clear that both methods produces well approximations to the solution of (4.3.8). In order to examine the accuracy of both numerical

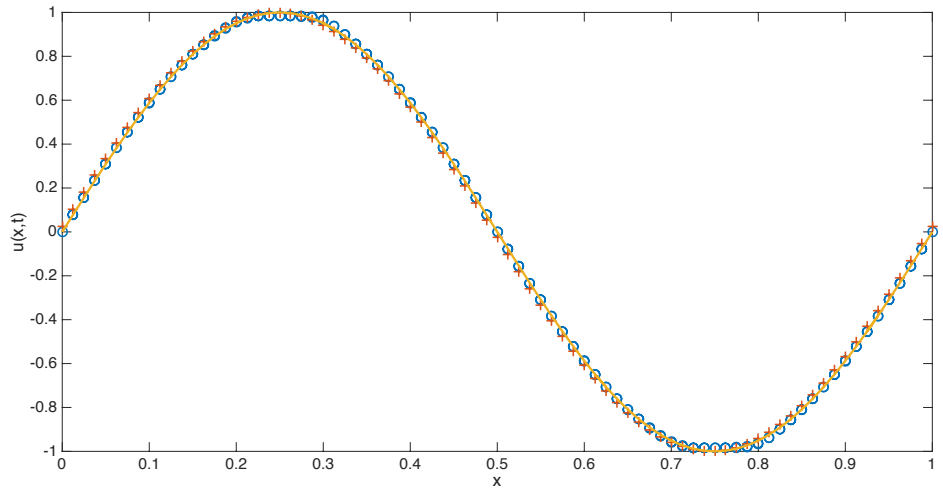

Figure 4.1: Transport equation - Solution at $T = 4.0$ for smooth initial condition and periodic boundary conditions with time-step $\Delta t = 10^{-4}$ and N=80 elements. The solid line represents the exact solution, 'o' line represents the 2nd-order RKDG approximate solution and the '+' line the 1st-order FV approximate solution.

schemes, we perform a convergence test. Firstly, we introduce the discrete L^2

norm to measure the error

$$\|u - u_h\|_{2,\Delta} = \sqrt{\Delta x_i \sum_i (u\big|_{I_i} - u_h\big|_{I_i})^2}, \tag{4.3.11}$$

where Δx_i is the length of cell I_i. Also, to estimate the rate of convergence, we assume that

$$\|u - u_h\|_{2,\Delta} = C\Delta {x_i}^p,$$

where p the rate of convergence. Due to the fact that finite volume methods produce approximations to the average of the solution in every cell, we compute the error of the averages of the solution to obtain comparable values between the two methods. Table 4.1 displays the discrete L^2 errors at T= 4.0 as a function of the number of elements and the rate of convergence for finite volume method and discontinuous Galerkin method with different polynomial orders. We ob-

N	FV	Rate	RKDG-r=1	Rate	RKDG-r=2	Rate
20	3.017799e-01		8.464073e-02		1.008654e-03	
40	7.472050e-02	2.0139	2.167689e-02	1.9652	1.744945e-04	2.5312
80	1.848853e-02	2.0149	5.287170e-03	2.0356	2.396353e-05	2.8643
100	1.180542e-02	2.0103	3.319720e-03	2.0857	1.209096e-05	3.0656

Table 4.1: Transport equation - Discrete L^2 errors of solution averages at $T = 4.0$ for smooth initial condition with time-step $\Delta t = 10^{-4}$.

serve that the increase of the accuracy of the discontinuous Galerkin method relies on the increase of either the number of elements or the polynomial order. Moreover, it is noticeable that the finite volume scheme has almost the same accuracy with the discontinuous Galerkin scheme using linear basis functions, although the finite volume scheme (3.2.10) is, in general, first order accurate. This is due to the super-convergence of finite volume schemes in symmetric intervals. For the discontinuous Galerkin cases, we observe that the rate of convergence $p \approx r + 1$, where r is the polynomial order, verifies the proposition

(4.1.1).

- Discontinuous initial condition:

  Recalling the problem (4.3.8), we now select the initial condition $u_0(x)$ to be a discontinuous function

$$u_0(x) = \begin{cases} 1.0, & -0.4 \leq x \leq 0.4, \\ 2.0, & \text{otherwise.} \end{cases} \tag{4.3.12}$$

  Therefore, the exact solution of (4.3.8) for $x \in [0,1], t \geq 0$ is

$$u(x,t) = \begin{cases} 1.0, & -0.4 \leq x - t \leq 0.4, \\ 2.0, & \text{otherwise.} \end{cases} \tag{4.3.13}$$

  Figure 4.2 displays the exact and numerical solutions of (4.3.8) with the initial condition (4.3.12) and periodic boundary conditions at $T = 0.4$. The numerical solutions were produced using a uniform mesh which consists of 80 cells I_i and a fixed time step of $\Delta t = 10^{-4}$. It is obvious that the limiting Runge-Kutta discontinuous Galerkin scheme (4.3.7) with linear polynomial functions gives more accurate results along the discontinuities than the finite volume scheme (3.2.10).

4.3.2 Inviscid Burger's equation

The inviscid Burger's equation is a popular example of nonlinear conservation law whose solution are discontinuous even for smooth initial conditions. Hence the numerical schemes (4.3.7) and (3.2.10) implemented in the previous chapter should

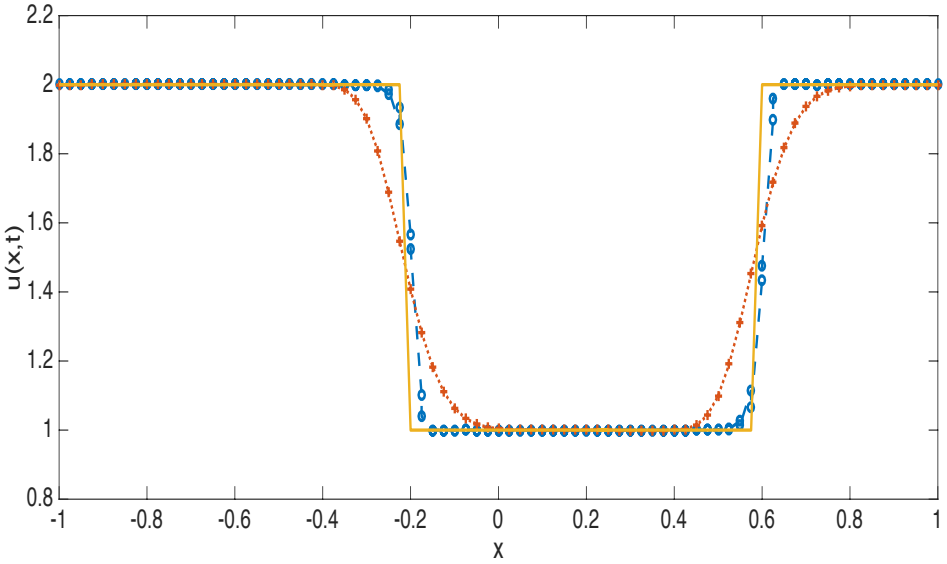

Figure 4.2: Transport equation - Solution at $T = 0.4$ for discontinuous initial condition and periodic boundary conditions with time-step $\Delta t = 10^{-4}$ and N=80 elements. The solid line represents the exact solution, the 'o' line represents the numerical solution of 2nd-order RKDG method and the '+' line the numerical solution of 1st-order FV method.

capture a solution that involves a shock. We consider the problem

$$\begin{cases} u_t + uu_x = 0, & x \in [-1,1], t \geq 0, \\ u(x,0) = \dfrac{1}{4} + \dfrac{1}{2}cos(\pi x), & x \in [-1,1]. \end{cases} \tag{4.3.14}$$

Firstly, we compute theoretically when the shock is formed. According to proposition (2.3.1) the shock of (4.3.14) occurs at time

$$T_b = \frac{-1}{\min_{x\in\mathbb{R}} u_0'(x))}. \tag{4.3.15}$$

Hence, we obtain

$$T_b = \frac{-1}{\min_{x\in\mathbb{R}} -\frac{1}{2}\pi sin(\pi x)} = \frac{2}{\pi}.$$

We introduce now a uniform mesh which consists of 100 cells I_i and a fixed time step of $\Delta t = 10^{-4}$. Figure 4.3 displays the approximations to solution of (4.3.14) with periodic boundary conditions at different time levels. We observe that away from the

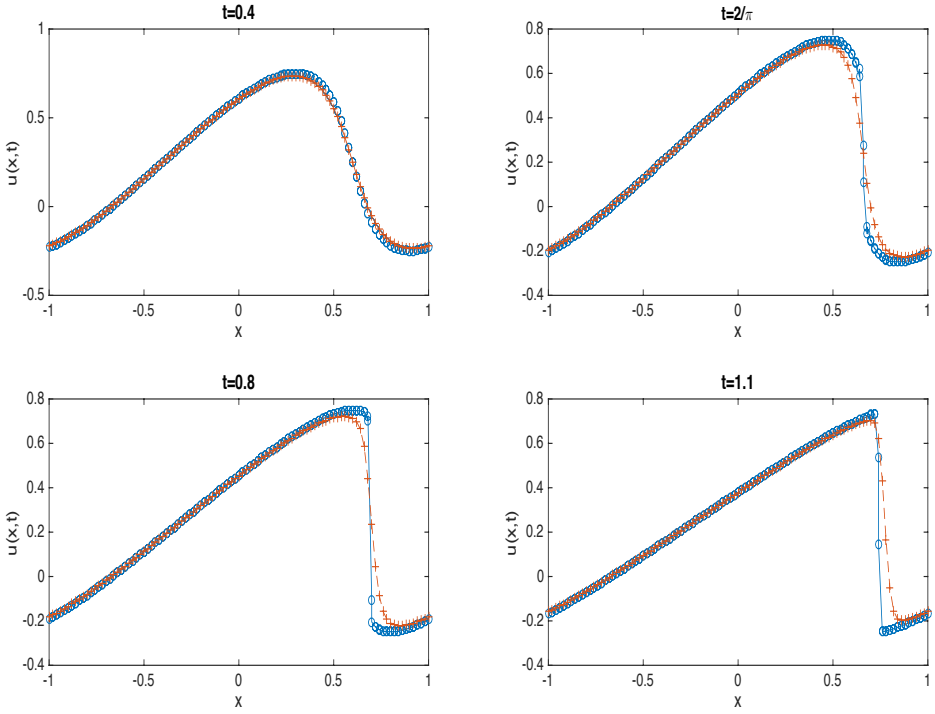

Figure 4.3: Burgers' equation - Solution at different time levels with time-step $\Delta t = 10^{-4}$ and N=100 elements. The 'o' line represents the numerical solution of 2nd-order RKDG method and the '+' line the numerical solution of 1st-order FV method.

shock where the solution is smooth, the approximate solutions produced by the two numerical schemes coincide. However, along the discontinuity when the shock occurs, the finite volume scheme smooths out the solution.

4.3.3 System of Elastodynamics

The system of elastodynamics arises from continuum physics and it describes the propagation of elastic waves in a medium. The system consists of two equations, a

linear and nonlinear conservation law

$$\begin{cases} u_t - v_x = 0, & x \in [-1,1], t \geq 0, \\ v_t - g(u)_x = 0, \end{cases} \tag{4.3.16}$$

where u is the shear-strain and v is the velocity. We select $g(u) = u + u^3$ and we impose appropriate initial conditions and periodic boundary conditions. We set

$$u_0(x) = \begin{cases} 1.0, & -0.5 \leq x \leq 0.5, \\ 2.0, & \text{otherwise}, \end{cases} \qquad \text{and} \qquad v_0(x) = 2.0. \tag{4.3.17}$$

Considering that the Lax-Friedrichs flux involves a constant which reflects the wave speed of the flux, we determine the wave speed of u and v. The wave speeds rely on the system (4.3.16) and they are considered as the eigenvalues of the Jacobian matrix of (4.3.16). If we rewrite (4.3.16) as

$$\frac{\partial}{\partial t}\begin{bmatrix} u \\ v \end{bmatrix} + \begin{bmatrix} 0 & -1 \\ -g'(u) & 0 \end{bmatrix} \frac{\partial}{\partial x}\begin{bmatrix} u \\ v \end{bmatrix} = 0, \tag{4.3.18}$$

then the Jacobian matrix J will be given by

$$J = \begin{bmatrix} 0 & -1 \\ -g'(u) & 0 \end{bmatrix},$$

and its eigenvalues will be $\lambda_{\pm} = \pm\sqrt{g'(u)}$. Hence, for this example, the eigenvalues are $\lambda_{\pm} = \pm\sqrt{1+3u^2}$ and thus the constant in the numerical flux is $\alpha = \sqrt{1+3u^2}$. To implement now the finite volume and the discontinuous Galerkin schemes for the system (4.3.16) with initial conditions (4.3.17), we introduce a uniform mesh which consists of 80 cells I_i and a fixed time step of $\Delta t = 10^{-4}$. Figure 4.4 demonstrates the approximations to solution of u and v at T=0.07. In comparison with the Runge-

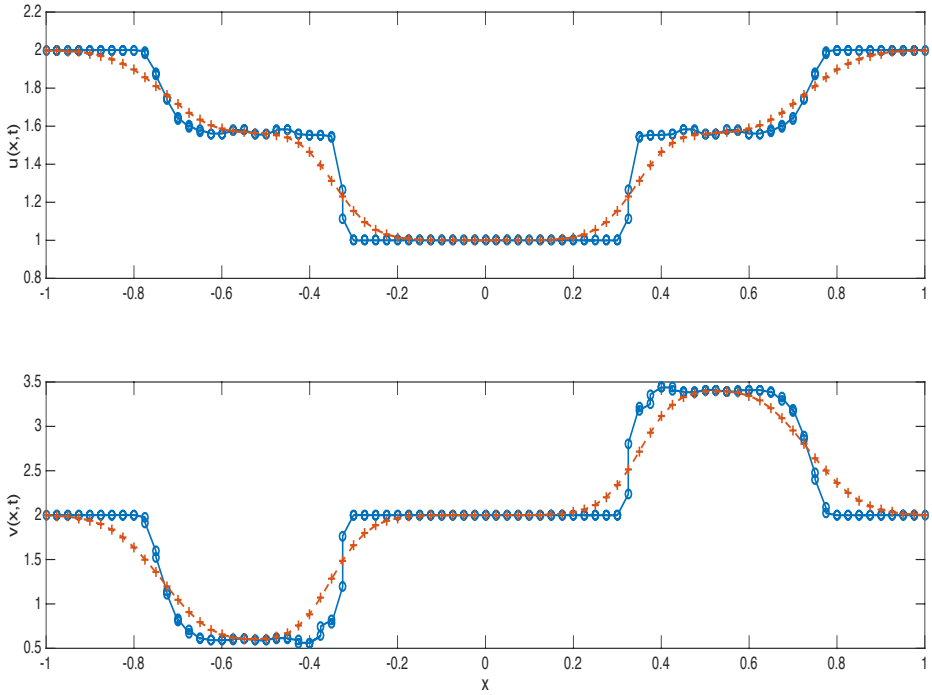

Figure 4.4: System of elastodynamics - Solution at T=0.07 with time-step $\Delta t = 10^{-4}$ and N=80 elements. The 'o' line represents the numerical solution of 2nd-order RKDG method and the '+' line the numerical solution of 1st-order FV method. The first graph displays the approximation to u and the second graph the approximation to v.

Kutta discontinuous Galerkin scheme, the finite volume scheme smooths out again the solution along the discontinuities.

REFERENCES

[1] C. M. Dafermos, *Hyperbolic Conservation Laws in Continuum Physics*, 3rd ed. Berlin: Springer-Verlag, 2010.

[2] P. D. Lax, *Hyperbolic Systems of Conservation Laws and the Mathematical Theory of Shock Waves*. Philadelphia: Society for Industrial and Applied Mathematics, 1973.

[3] R. J. LeVeque, *Numerical Methods for Conservation Laws*, 2nd ed., ser. Lectures in Mathematics ETH Zurich. Basel: Springer Basel AG, 1992.

[4] ——, *Finite Volume Methods for Hyperbolic Problems*. Cambridge: Cambridge University Press, 2002.

[5] C. W. Shu, "Numerical Methods for Hyperbolic Conservation Laws," Lecture Notes, 2006.

[6] B. Szabo and I. Babuska, *Introduction to Finite Element Analysis*. Sussex: Wiley, 2011.

[7] W. Reed and T.R.Hill, "Triangular Mesh Method for the Neutron Transport Equation," Los Alamos Scientific Laboratory, LA-UR-73-479, 1973.

[8] G. Chavent and G. Salzano, "A Finite Element Method for 1-D Water Flooding Problem with Gravity," *Journal of Computational Physics*, vol. 45, no. 3, pp. 307–344, 1982.

[9] G. Chavent and B. Cockburn, "The Local Projection P0P1 - Discontinuous Galerkin Finite Element Method for Scalar Conservation Laws," *RAIRO Mathematical Modelling and Numerical Analysis*, vol. 23, no. 4, pp. 565–592, 1989.

[10] B. Cockburn and C. W. Shu, "The Runge-Kutta Local Projection P1 - Discontinuous Galerkin Finite Element Method for Scalar Conservation Laws," *RAIRO Mathematical Modelling and Numerical Analysis*, vol. 3, no. 25, pp. 337–361, 1989.

[11] ——, "TVB Runge-Kutta Local Projection Discontinuous Galerkin Finite Element Method for Conservation Laws II: General Framework," *Mathematics of Computation*, vol. 52, no. 186, pp. 411–435, 1989.

[12] ——, "The Runge-Kutta Discontinuous Galerkin Methods for Conservation Laws V: Multidimensional Systems," *Journal of Computational Physics*, vol. 141, no. 2, pp. 199–224, 1998.

[13] R. Biswas, K. D. Devine, and J. E. Flaheerty, "Parallel, Adaptive Finite Element Methods for Conservation Laws," *Applied Numerical Mathematics*, vol. 14, no. 1-3, pp. 255–283, 1994.

[14] J. E. Flaheerty, L. Krivodonova, J.-F. Remacle, and M. S. Shephard, "Aspects of Discontinuous Galerkin Methods for Hyperbolic Conservation Laws," *Finite Element Analysis and Design*, vol. 38, no. 10, pp. 889–908, 2002.

[15] J. Qiu and C. W. Shu, "Runge-Kutta Discontinuous Galerkin Method Using WENO Limiters," *Siam Journal Scientific Computing*, vol. 26, no. 3, pp. 907–929, 2005.

[16] H. Luo, J. D. Baum, and R. Lohner, "A Hermite WENO-Based Limiter for Discontinuous Galerkin Method on Unstructured Grids," *Journal of Computational Physics*, vol. 225, no. 1, 686-713 2006.

[17] B. Cockburn and C. W. Shu, "The Local Discontinuous Galerkin Method for Time-Dependent Convection-Diffusion Systems," *Siam Journal Numerical Analysis*, vol. 35, no. 6, pp. 2440–2463, 1998.

[18] B. Cockburn, J. Gopalakrishnan, and R. Lazarov, "Unified Hybridization of Discontinuous Galerkin, Mixed, and Continuous Galerkin Methods for Second Order Elliptic Problems," *Siam Journal Numerical Analysis*, vol. 47, no. 2, pp. 1319–1365, 2009.

[19] J. M. Burgers, "A Mathematical Model Illustrating the Theory of Turbulence," in *Advances in Applies Mechanics*. New York: Academic Press, 1948.

[20] O. Oleinik, *Discontinuous Solutions of Nonlinear Differential Equations*, ser. 2. American Mathematic Society Translation, 1957.

[21] J. Smoller, *Shock Waves and Reaction-Diffusion Equations*, 2nd ed. Springer, 1994, ch. The Single Conservation Law.

[22] E. Godlewski and P.-A. Raviart, *Numerical approximation of hyperbolic systems of conservation laws*. New York: Springer-Verlag, 1996.

[23] C. W. Shu, "Discontinuous Galerkin Methods: General Approach and Stability," in *Numerical Solutions of Partial Differential Equations*, ser. Advanced Courses in Mathematics CRM Barcelona. Basel: Birkhauser, 2009.

[24] ——, "Discontinuous Galerkin Methods for Time-Dependent Problems: Survey and Recent Developments," in *Recent Developments in Discontinuous Galerkin Finite Element Methods for Partial Differential Equations*, ser. 2012 John H Barret Memorial Lectures, X. Feng, O. Karakashian, and Y. Xing, Eds. Basel: Springer, 2014.

[25] X. Meng, C. W. Shu, Q. Zhang, and B. Wu, "Superconvergence of Discontinuous Galerkin Methods for Scalar Nonlinear Conservation Laws in One Space Dimension," *Siam Journal Numerical Analysis*, vol. 50, no. 5, pp. 2336–2356, 2012.

[26] Y. Cheng and C. W. Shu, "Superconvergence and Time Evolution of Discontinuous Galerkin Finite Element Solutions," *Journal of Computational Physics*, no. 227, pp. 9612–9627, 2008.

[27] G. Jiang and C. W. Shu, "On a Cell Entropy Inequality for Discontinuous Galerkin Methods," *Mathematics of Computation*, vol. 62, no. 206, pp. 531–538, 1994.

[28] B. Cockburn, C. W. Shu, and T. Eitan, *Advanced Numerical Approximation of Nonlinear Hyperbolic Equations*, ser. Lecture notes in Mathematics. Springer, 1998, ch. Discontinuous Galerkin Methods.

[29] R. J. LeVeque, *Finite Difference Methods for Ordinary and Partial Differential Equations : Steady-State and Time-Dependent Problems.* Society for Industrial and Applied Mathematics, 1995, ch. Advection Equations and Hyperbolic Systems.

APPENDIX

A Finite Element Method for Hyperbolic Conservation Laws

In Section 3.3, it was stated that the finite element method in its classical form cannot be used for solving hyperbolic conservation laws because its applications leads to nonconservative methods which can be also unstable. For example, in the case of approximating the solution of a hyperbolic conservation law using piecewise linear functions, the finite element method is equivalent to the corresponding central finite difference method which is unstable. Here we explain why this observation is true. For simplicity of the presentation, we develop the method on a simple linear transport equation.

We consider the Cauchy problem

$$\begin{cases} u_t + \alpha u_x = 0, & x \in [a,b], t \geq 0, \\ u(x,0) = u_0(x). \end{cases} \tag{A.0.1}$$

where $\alpha \in \mathbb{R}$. Let $\mathcal{T}$ be a uniform partition of [a,b] consisting of N subintervals $I_i = [x_i, x_{i+1}]$ of fixed length Δx. Denote

$$\Delta x = \frac{b-a}{N},$$
$$x_i = a + i\Delta x, \quad i = 0, 1, \ldots, N$$

In order to apply the finite element method to the problem (A.0.1), we start with deriving its weak formulation. Let v be a test function. We multiply (A.0.1) by v,

integrate over $[a, b]$ and do integration by parts

$$\begin{aligned} 0 &= \int_a^b (u_t + \alpha u_x)\, v\, dx \\ &= \int_a^b u_t v\, dx + \int_a^b \alpha u_x v\, dx \\ &= \int_a^b u_t v\, dx + \alpha uv\Big|_a^b - \int_a^b \alpha u v'\, dx. \end{aligned} \tag{A.0.2}$$

We impose the following boundary conditions

$$u(a, t) = u(b, t) = 0, \qquad t \geq 0.$$

Then from (A.0.2) we obtain

$$\int_a^b u_t v\, dx - \int_a^b \alpha u v'\, dx = 0.$$

This motivates us to define a finite dimensional space consisting of linear piecewise polynomials

$$V_h = \{v \in L^2([a, b]) : v|_{I_i} \in \mathbb{P}(I_i)\},$$

where $\mathbb{P}$ is the set of liner polynomials. Thus, the finite element method is defined as follows: we seek $u_h \in V_h$ an approximate solution of (A.0.1), that satisfies

$$\int_a^b (u_h)_t \phi\, dx - \alpha \int_a^b u_h \phi'\, dx = 0, \qquad \forall \phi \in V_h, \tag{A.0.3}$$

Let $\phi_1, \phi_2, \ldots, \phi_{N_h}$ be a basis of V_h. We set $\{\phi_i\}_{i=1}^{N_h}$ the linear Lagrange polynomials, i.e. for $i = 1, \ldots, N_h$

$$\phi_i(x) = \begin{cases} \dfrac{x - x_{i-1}}{\Delta x}, & x_{i-1} \leq x \leq x_i, \\ \dfrac{x_{i+1} - x}{\Delta x}, & x_i \leq x \leq x_{i+1}, \\ 0, & \text{otherwise.} \end{cases} \tag{A.0.4}$$

Therefore, we can define u_h as linear combinations of ϕ_j

$$u_h = \sum_{j=1}^{N_h} u_j \phi_j(x), \tag{A.0.5}$$

where the set of coefficients u_j need to be determined. In addition, the test function ϕ can be considered as one of the basis functions, i.e. $\phi \in \{\phi_i\}_{i=1}^{N_h}$. Suppose $\phi = \phi_l$, $l = 1, \ldots, N_h$. Then (A.0.3) yields

$$\int_a^b \left[\sum_{j=0}^{N_h} u_j \phi_j \right]_t \phi_l \, dx = \alpha \int_a^b \left[\sum_{j=0}^{N_h} u_j \phi_j \right] \phi_l' \, dx, \qquad l = 0, \ldots, r,$$

or

$$\sum_{j=0}^{N_h} \dot{u_j} \left[\int_a^b \phi_j \phi_l \, dx \right] = \alpha \sum_{j=0}^{N_h} u_j \left[\int_a^b \phi_j \phi_l' \, dx \right], \tag{A.0.6}$$

where $\dot{u_j}$ denotes the time derivative. A fully discrete scheme of (A.0.6) can be derived using an approximation of the time derivative $\dot{u_j}$, with the simplest being the forward Euler method

$$u_t(x, t_n) \approx \frac{U^{n+1} - U^n}{\Delta t}.$$

Therefore, a fully discrete approximation is defined as follows: find $u_h \in V_h^r$ such that $\forall l$

$$\sum_{j=0}^{N_h} \frac{U_j^{n+1} - U_j^n}{\Delta t} \left[\int_a^b \phi_j \phi_l \, dx \right] = \alpha \sum_{j=0}^{N_h} U_j^n \left[\int_a^b \phi_j \phi_l' \, dx \right],$$

or

$$\sum_{j=0}^{N_h} U_j^{n+1} \left[\int_a^b \phi_j \phi_l \, dx \right] = \sum_{j=0}^{N_h} U_j^n \left[\int_a^b \phi_j \phi_l \, dx \right] + \alpha \Delta t \sum_{j=0}^{N_h} U_j^n \left[\int_a^b \phi_j \phi_l' \, dx \right]. \tag{A.0.7}$$

We observe that (A.0.7) is a linear system and it is written in a matrix form

$$GU^{n+1} = GU^n + \alpha \Delta t S^T U^n, \tag{A.0.8}$$

where G is referred as mass matrix, S is referred as stiffness matrix and U^n is the vector of unknowns and

$$G = \begin{bmatrix} \int_a^b \phi_1\phi_1 dx & \cdots & \int_a^b \phi_1\phi_{N_h} dx \\ \vdots & \ddots & \vdots \\ \int_a^b \phi_{N_h}\phi_1 dx & \cdots & \int_a^b \phi_{N_h}\phi_{N_h} dx \end{bmatrix}, S = \begin{bmatrix} \int_a^b \phi_1\phi_1' dx & \cdots & \int_a^b \phi_1\phi_{N_h}' dx \\ \vdots & \ddots & \vdots \\ \int_a^b \phi_{N_h}\phi_1' dx & \cdots & \int_a^b \phi_{N_h}\phi_{N_h}' dx \end{bmatrix}, U^n = \begin{bmatrix} u_1^n \\ \vdots \\ u_{N_h}^n \end{bmatrix}.$$

Considering that the basis functions are linear Lagrange polynomials which have support with 2 subintervals, it follows that both matrices G and S are tridiagonal. Motivated from (A.0.4), we can compute the non-zero entries of these matrices. Let's start with the mass matrix G.

$$G_{ii} = \int_a^b \phi_i\phi_i\, dx = \int_{x_{i-1}}^{x_i} \left(\frac{x - x_{i-1}}{\Delta x}\right)^2 dx + \int_{x_i}^{x_{i+1}} \left(\frac{x_{i+1} - x}{\Delta x}\right)^2 dx = \frac{\Delta x}{3} + \frac{\Delta x}{3} = \frac{2\Delta x}{3},$$
$$G_{i,i-1} = \int_a^b \phi_i\phi_{i-1}\, dx = \int_{x_{i-1}}^{x_i} \frac{x_i - x}{\Delta x}\frac{x_i - x}{\Delta x}\, dx = \frac{\Delta x}{6},$$
$$G_{i,i+1} = \int_a^b \phi_i\phi_{i+1}\, dx = \int_{x_i}^{x_{i+1}} \frac{x_{i+1} - x}{\Delta x}\frac{x - x_i}{\Delta x}\, dx = \frac{\Delta x}{6},$$

where G_{ii} are the diagonal entries, $G_{i,i-1}$ the entries below the diagonal and $G_{i,i+1}$ the entries above. So, the matrix G becomes

$$G = \begin{bmatrix} \frac{2\Delta x}{3} & \frac{\Delta x}{6} & & \frac{\Delta x}{6} & \\ \frac{\Delta x}{6} & \frac{2\Delta x}{3} & \frac{\Delta x}{6} & & \\ & \ddots & \ddots & \ddots & \\ & & \frac{\Delta x}{6} & \frac{2\Delta x}{3} & \frac{\Delta x}{6} \\ \frac{\Delta x}{6} & & & \frac{\Delta x}{6} & \frac{2\Delta x}{3} \end{bmatrix} = \Delta x \begin{bmatrix} \frac{2}{3} & \frac{1}{6} & & \frac{1}{6} & \\ \frac{1}{6} & \frac{2}{3} & \frac{1}{6} & & \\ & \ddots & \ddots & \ddots & \\ & & \frac{1}{6} & \frac{2}{3} & \frac{1}{6} \\ \frac{1}{6} & & & \frac{1}{6} & \frac{2}{3} \end{bmatrix} = \Delta x\, \tilde{G}.$$

We consider now the matrix S. Then, the non-zero entries of S are

$$S_{ii} = \int_{x_{i-1}}^{x_{i+1}} \phi_i\phi_i'\, dx = \int_{x_{i-1}}^{x_i} \frac{x - x_{i-1}}{\Delta x}\frac{1}{\Delta x}\, dx + \int_{x_i}^{x_{i+1}} \frac{x_{i+1} - x}{\Delta x}\frac{-1}{\Delta x}\, dx = \frac{1}{2} - \frac{1}{2} = 0,$$

$$S_{i,i-1} = \int_a^b \phi_i \phi'_{i-1}\, dx = \int_{x_{i-1}}^{x_i} \frac{x_i - x}{\Delta x} \frac{-1}{\Delta x}\, dx = -\frac{1}{2},$$
$$S_{i,i+1} = \int_a^b \phi_i \phi'_{i+1}\, dx = \int_{x_i}^{x_{i+1}} \frac{x - x_i}{\Delta x} \frac{1}{\Delta x}\, dx = \frac{1}{2},$$

where S_{ii} are the diagonal entries, $S_{i,i-1}$ the entries below the diagonal and $S_{i,i+1}$ the entries above. Hence, the matrix S is defined as follows

$$S = \frac{1}{2}\begin{bmatrix} 0 & 1 & & -1 & \\ -1 & 0 & 1 & & \\ & \ddots & \ddots & \ddots & \\ & & -1 & 0 & 1 \\ 1 & & & -1 & 0 \end{bmatrix}$$

and it is obvious that $S^T = -S$. Consequently, we can rewrite the system (A.0.8) as

$$\Delta x\, \tilde{G} U^{n+1} = \Delta x\, \tilde{G} U^n - \alpha \Delta t S U^n,$$

$$\tilde{G} U^{n+1} = \tilde{G} U^n - \alpha \frac{\Delta t}{\Delta x} S U^n. \tag{A.0.9}$$

In order to examine if the finite element method is equivalent to the corresponding central finite difference method, we introduce the finite difference scheme for (A.0.1). Using central differences in space and forward Euler in time, we obtain

$$U_j^{n+1} = U_j^n - \frac{\alpha}{2} \frac{\Delta t}{\Delta x} (U_{j+1}^n - U_{j-1}^n). \tag{A.0.10}$$

We notice that the discretisation (A.0.9) of the differential operator u_x by the finite element method is the same with that of the central difference scheme (A.0.10). Due to instability of the central finite difference method [29], we finally conclude that finite element method for hyperbolic conservation laws is also unstable.